COO-2245-22TR
Distribution Category UC-79e

# TURBULENT MOMENTUM EXCHANGE COEFFICIENTS FOR REACTOR FUEL BUNDLE ANALYSIS

by

H. Ninokata and N.E. Todreas

June, 1975

DEPARTMENT OF NUCLEAR ENGINEERING

MASSACHUSETTS INSTITUTE OF TECHNOLOGY

Cambridge, Massachusetts

02139

NOTICE

This report was prepared as an account of work sponsored by the United States Government. Neither the United States nor the United States Energy Research and Development Administration, nor any of their employees, nor any of their contractors, subcontractors, or their employees, makes any warranty, express or implied, or assumes any legal liability or responsibility for the accuracy, completeness or usefulness of any information, apparatus, product or process disclosed, or represents that its use would not infringe privately owned rights.

ERDA Research and Development
Contract AT(11-1)-2245
U.S. Energy Research and Development Administration

DISTRIBUTION OF THIS DOCUMENT UNLIMITED

## DISCLAIMER

This report was prepared as an account of work sponsored by an agency of the United States Government. Neither the United States Government nor any agency Thereof, nor any of their employees, makes any warranty, express or implied, or assumes any legal liability or responsibility for the accuracy, completeness, or usefulness of any information, apparatus, product, or process disclosed, or represents that its use would not infringe privately owned rights. Reference herein to any specific commercial product, process, or service by trade name, trademark, manufacturer, or otherwise does not necessarily constitute or imply its endorsement, recommendation, or favoring by the United States Government or any agency thereof. The views and opinions of authors expressed herein do not necessarily state or reflect those of the United States Government or any agency thereof.

## DISCLAIMER

Portions of this document may be illegible in electronic image products. Images are produced from the best available original document.

CONTENTS

## Abstract

A unified treatment of the turbulent and the molecular effects on the mixing coefficients has been performed and the momentum exchange coefficient $\overline{W_{ij}^{*M}}$ evaluated for small triangular array rod bundles (19 pins and 37 pins) without spacers. These results are based on the output of the computer code "VELASCO" which performs the calculation of the velocity distribution within a fuel rod array. The results show that momentum exchange coefficients vary considerably with spatial position in the bundle. A method for deriving energy exchange coefficients as input data for COBRA analysis is presented. These energy exchange coefficients can be calculated by the method of this report when VELASCO or a similar distributed parameter code is developed to compute thermal fields within a fuel rod array.

Acknowledgement

The authors gratefully express their thankfulness to Mrs. Virginia O'Keefe and Miss K. Nozawa for their typing. This work was supported by the USAEC under Contract AT(11-1)-2245.

LIST OF TABLES

## LIST OF FIGURES

Figure No. | Page

Nomenclature

| | |
|---|---|
| b,c | width of open channel (i.e., gap) |
| $c_p$ | specific heat |
| D | diameter of a fuel pin |
| $G_i$ | mass velocity in i-th subchannel |
| h | mesh size |
| $\overline{L}^{*M}_{ij}$ | momentum mixing length scale |
| $M_{ij}$ | mixing Stanton number |
| P | pitch |
| Pe | peripheral length of the symmetry of the wetted duct wall (note in VELASCO sometimes pin wall is used) |
| PW | twice distance from wall to rod center |
| q | energy |
| $\overline{q'_{ij}}$ | energy corssing gap per unit axial length per unit |
| $\overline{q''_{ij}}$ | energy or heat flux $(\frac{\text{energy}}{\text{area time}})$ |
| R | fuel radius |
| r | radial distance from the center of fuel |
| $r_m$ | radial distance from the center of fuel to zero sheat stress line |
| T | temperature |
| $\overline{T}_i$, $\overline{T}_j$ | $i^{th}/j^{th}$ subchannel temperature |
| UB(TOT) | bundle average velocity |
| u | dimensionless velocity, made dimensionless by division of local velocity by UB(TOT) |
| $\nabla u$ | gradient of dimensionless velocity |

| | |
|---|---|
| $\overline{V}_i$, $\overline{V}_j$, $UB_i$ | $i^{th}/j^{th}$ subchannel velocity |
| $V_i$ | normalized i-th subchannel velocity ($=UB_i/UB(TOT)$) |
| $v$ | coolant velocity, subscripts $r$, $\phi$, $z$ denote radial, peripheral and axial components respectively. |
| $v'$ | fluctuation of coolant velocity |
| $\overline{W_{ij}^{*M}}$ | momentum exchange coefficient between subchannel i and j |
| $Y_{ij}$ | length between two adjacent subchannel centroids |
| $Z_{ij}^{*M}$ | mixing distance (1/cm) |
| $\beta$ | mixing Stanton number as used by Rowe and Angle (Ref. 7) |
| $\beta^*$ | relative momentum mixing Stanton number (Eqn. 3.15.b) |
| $\varepsilon^M$ | eddy diffusivity of momentum, subscripts $r\phi$, $\phi\phi$, $z\phi$ denoting components. |
| $\varepsilon_\phi$ | Eqn. 3.8.b |
| $\mu$ | viscosity of coolant |
| $\nu$ | dynamic viscosity of coolant |
| $\xi$ | r/R |
| $\rho$ | density of coolant |
| $\tau$ | shear stress tensor |
| $\overline{\tau_{ij}}$ | momentum flux $(\frac{momentum}{area\ time})$ |
| $\overline{\tau'_{ij}}$ | momentum crossing gap per unit axial length per unit time $(\frac{momentum}{length\ time})$ (equal $\tau_{ij}$ per Eqn. 3.5) |

GENERAL COMMENTS

1. Velocities are normalized by an overall channel averaged bulk velocity at $Re=10^5$ of nineteen and thirty seven rod bundles respectively. Hence the gradient of the velocity and the momentum mixing Stanton number are given in relative values.

2. Mixing distances and momentum exchange coefficients are given in actual values.

3. Material properties are those of Na at 700°C.

4. P/D = 1.25, and PW/D = 1.15.

## 1. Introduction

It is known that the lumped parameter approach is a useful mathematical method if the appropriate momentum and heat transfer length scales associated with diffusion phenomena are employed. Here, attention is focused on the exchange coefficients $\overline{W_{ij}^{*M}}$ [Ref. 1] within a multichannel region divided into a certain number of subchannels (Fig. 1 to 3), since these quantities play an important role in solving momentum balance equations used in lumped parameter systems [Ref. 2 and 3]. The subchannels near the fuel assembly duct wall are of particular interest for thermal-hydraulic design, since the non-uniformity in geometry and flow conditions may provoke important circumferential cladding temperature variations, causing excessive thermal stresses or leading to bowing of outer rods.

## 2. Problem Definition and General Method of Solution

This paper deals with prediction of momentum exchange coefficients $\overline{W_{ij}^{*M}}$ along every subchannel boundary in a hexagonal rod bundle configuration. First momentum exchange coefficients are obtained as a function of radial distance from the wall of fuel pin or duct of channel. Second these distributed values are averaged along the boundary to give an overall momentum exchange coefficients $\overline{W_{ij}^{*M}}$ between two subchannels. Attention will be primarily paid to the edge channels and on the spatial dependency of $\overline{W_{ij}^{*M}}$ in a bundle containing N pins.

The method of obtaining $\overline{W_{ij}^{*M}}$ is extraporated from Appendix A of [Ref. 1] and will be shown in Chapter 3. The VELASCO code has been used in the numerical application of this method which restricts the present results to symmetric bare rod configurations with fully developed, turbulent flow and limited secondary flow consideration. Furthermore, since VELASCO employs some basic assumptions and general expressions for the radial distribution of axial velocity (see Appendix A and Ref. 4 or Ref. 5 for the details) it should be noticed that the momentum mixing is calculated based on a velocity distribution given by VELASCO, not on a momentum balance equation itself. In spite of these limitations, the result should be a good prediction of the spatial variation of exchange coefficients and will provide users of subchannel analysis code with alternate and possible better input data than from empirical approaches.

Minor changes have been made to "VELASCO" and are shown in Appendix B.

## 3. Specific Method of Solution

### 3.1 Definitions and Formulation

The following assumptions have been made in the formulation of the problem.

3.1.1 Flow is incompressible

3.1.2 Fluid properties are independent of temperature

3.1.3 Steady state exists

3.1.4 Fully developed flow

3.1.5 $\frac{\partial}{\partial r}\left(\frac{v_\phi}{r}\right)$, $\frac{\partial v_r}{\partial \phi}$, $\frac{\partial v_\phi}{\partial \phi}$, $v_r$, $\overline{v_r' v_\phi'}$, $\overline{v_\phi' v_\phi'}$ are negligible compared with the $\frac{\partial v_z}{\partial \phi}$ at the angle, $\phi$=o, of interest.

With these assumptions, and remembering that our interests lie in a momentum cross flow across the subchannel boundary, the three $\phi$-components of the nine shear stress tensor components will be written as

$$= \begin{bmatrix} \tau_{r\phi} \\ \tau_{\phi\phi} \\ \tau_{z\phi} \end{bmatrix}$$

$$= \begin{bmatrix} o \\ o \\ \tau_{z\phi} \end{bmatrix}$$

$$= \begin{bmatrix} o \\ o \\ -\mu\frac{1}{r}\frac{\partial v_z}{\partial \phi} + \rho\, \overline{v_z' v_\phi'} \end{bmatrix} \quad \text{without transport by secondary flow.} \qquad (3.1.a)$$

$$= \begin{bmatrix} o \\ o \\ -\mu\frac{1}{r}\frac{\partial v_z}{\partial \phi} + \rho \overline{v_z' v_\phi'} + \rho v_z v_\phi \end{bmatrix} \quad \text{with transport by secondary flow.} \qquad (3.1.b)$$

In view of the Boussinesque approach, the eddy diffusivity of momentum has a tensor property. For example, the turbulent momentum flow in $\phi$-direction through each r, $\phi$ , z = constant plane is related to velocity gradient by eddy diffusivities

$\varepsilon^M_{r\phi}$, $\varepsilon^M_{\phi\phi}$, $\varepsilon^M_{z\phi}$ respectively. From the assumption 3.1.5, we presume $\varepsilon^M_{r\phi}$, $\varepsilon^M_{\phi\phi} \cong 0$ in this chapter. Then

$$\rho \, v_\phi' v_z' = -\rho \varepsilon^M_{z\phi} \frac{1}{r} \frac{\partial v_z}{\partial \phi} \tag{3.2}$$

Therefore, (3.1a, b) become

$$= \begin{bmatrix} 0 \\ 0 \\ -(\mu + \rho \varepsilon^M_{z\phi}) \frac{1}{r} \frac{\partial v_z}{\partial \phi} \end{bmatrix} \tag{3.3.a}$$

and

$$= \begin{bmatrix} 0 \\ 0 \\ -(\mu + \rho \varepsilon^M_{z\phi}) \frac{1}{r} \frac{\partial v_z}{\partial \phi} + \rho \, v_z v_\phi \end{bmatrix} \tag{3.3.b}$$

From now on throughout this paper, we simply denote the tensor quantity $\tau_\phi$ as

$$\tau_\phi = -(\mu + \rho \varepsilon^M_{z\phi}) \frac{1}{r} \frac{\partial v_z}{\partial \phi} \tag{3.4.a}$$

or

$$\tau_\phi = -(\mu + \rho \varepsilon^M_{z\phi}) \frac{1}{r} \frac{\partial v_z}{\partial \phi} + \rho \, v_z v_\phi \tag{3.4.b}$$

as if $\tau_\phi$ is a scalar quantity.

The total momentum cross flow across the boundary between i-th and j-th subchannels in the interior region (the exterior region results will be given later in this chapter) by molecular and turbulent transport is

$$\tau_{ij} = \int_b \tau_\phi(r) dr \tag{3.5}$$

where $\phi$ is the angle of boundary position and the integration is made over the length of subchannel boundary, b, which will change with position in the bundle or with bundle distortion. Only for interior channels of normal geometry bundles does b = P-D. A linearly averaged momentum cross flow is

$$\bar{\tau}_{ij} = \tau_{ij}/b \qquad (3.6)$$

We now proceed to introduce definitions analogous to the definitions of [ 1 ] for energy exchange, i.e.,

$$\overline{\tau'_{ij}} = b\,\overline{\tau}_{ij} \qquad (3.7.a)$$

analogous to

$$\bar{q}'_{ij} \doteq (P-D)\bar{q}''_{ij} \qquad \text{(following A.4 Ref. 1)}$$

where it should be noted $\bar{\tau}_{ij}$ and $\bar{q}''_{ij}$ are momentum fluxes and $\bar{\tau}'_{ij}$ and $\bar{q}'_{ij}$ are momentum and energy quantities crossing the subchannel boundary per unit axial length per unit time. The "'" notation used here by convention represents "per unit length" and should not be confused with the "'" notation referred to immediately below which represents instantaneous time values.

The momentum mixing flow rate, $\overline{W^{*M}_{ij}}$, is analogous to the energy mixing flow rate $\overline{W^{*H}_{ij}}$. Similarly the nomenclature $\overline{W^{*M}_{ij}}$ has been introduced in place of the more common notation $W'_{ij}$ of Ref. 5 to clearly indicate

(1) by "*" versus "'" that the mixing flow rate is due to both molecular and eddy effects rather than eddy effects only.

(2) by "M" that $\overline{W^{*M}_{ij}}$ is an effective hypothetical flow rate for momentum exchange versus mass or energy exchange.

(3) by "___" that the mixing flow rate is radially averaged along the subchannel boundary.

The momentum mixing flow rate $\overline{W^{*M}_{ij}}$ is expressed in terms of subchannel bulk velocity $\overline{V}_i$ and $\overline{V}_j$. Thus $\overline{W^{*M}_{ij}}$ plays the role of the parameter with regard to momentum transfer which is determined from distributed parameter methods to give more precise input information to the existing lumped parameter thermal-hydraulic codes. The defining equation for $\overline{W^{*M}_{ij}}$ then becomes

$$\overline{\tau}'_{ij} \equiv \overline{W^{*M}_{ij}} \, (\overline{V}_j - \overline{V}_i) \qquad (3.7.b)$$

analogous to

$$\overline{q'_{ij}} \equiv \overline{W^{*H}_{ij}} \, c_p(\overline{T}_i - \overline{T}_j) \qquad (A.11 \text{ Ref. } 1)$$

Substituting results of Eqns. 3.7.a , 3.6, 3.5 and 3.4.a, Eqn. 3.7.b becomes:

$$\overline{W^{*M}_{ij}} = \frac{\overline{\tau_{ij}}'}{\overline{V}_j - \overline{V}_i} \equiv \frac{b\overline{\tau_{ij}}}{\overline{V}_j - \overline{V}_i} = \frac{\int_b \tau(r)dr}{\overline{V}_j - \overline{V}_i}$$

$$= \frac{-\mu \int_{\frac{b}{R}} \left(1 + \frac{\varepsilon^M_{z\phi}}{\nu}\right) \frac{1}{\xi} \frac{\partial v_z}{\partial \phi} \, d\xi}{(\overline{V}_j - \overline{V}_i)} \qquad (3.8.a)$$

where the length scale r has been nondimensionalized by division by R yielding $\xi \equiv \frac{r}{R}$ .

Note that in 3.8.a we have expressed the gradient and $d\xi$ in cylindrical coordinates for convenience -- the generalized expressions should be $\nabla v_z$ and $d\mathbf{r}$.

Equation 3.8.a is an exact expression for $\overline{W_{ij}^{*M}}$ where the eddy diffusivity is a function of radius r (or $\xi$). In VELASCO, Eifler and Nijsing used a correlation

$$\varepsilon_\phi = 0.154 \sqrt{\frac{\tau_R}{\rho}} \, (r_m - R) \qquad (3.8.b)$$

where $r_m$ is the distance of zero shear stress line from the outer of the fuel pin. Then in this paper, we can consider $\varepsilon_\phi$ as constant along the subchannel boundary, Eqn. (3.8.a) will reduce to

$$\overline{W_{ij}^{*M}} = -\mu \left(1 + \frac{\varepsilon_{z\phi}^M}{\nu}\right) \int_{b/R} \frac{1}{\xi} \frac{\partial v_z}{\partial \phi} \, d\xi / (\overline{V}_j - \overline{V}_i) \qquad (3.8.c)$$

If we further work with the assumption that a radially averaged, circumferential gap velocity gradient is satisfactory we can further simplify the result below:

$$\overline{W_{ij}^{*M}} = -\mu \frac{b}{R} \left(1 + \frac{\varepsilon_{z\phi}^M}{\nu}\right) \overline{\frac{1}{\xi} \frac{\partial v_z}{\partial \phi}} \, / \, (\overline{V}_j - \overline{V}_i) \qquad (3.8.d)$$

The definition of momentum mixing length scale $\overline{L_{ij}^{*M}}$ is

$$\overline{L_{ij}^{*M}} = \frac{\overline{V}_j - \overline{V}_i}{\frac{Y_{ij}}{R} \overline{\frac{1}{\xi} \frac{\partial v_z}{\partial \phi}}} \qquad (3.9)$$

where $Y_{ij}$ is length between two adjacent subchannel centroids,

$\overline{\frac{1}{\xi}\frac{\partial v_z}{\partial \phi}}$ is an average of velocity gradients along the open subchannel boundary.

Combining (3.8.d) and (3.9), the following is obtained,

$$\overline{W^{*M}_{ij}} = -\mu \frac{b}{R} \left(1 + \frac{\varepsilon^M_{z\phi}}{\nu}\right) \frac{R}{\overline{L^{*M}_{ij}}\, Y_{ij}} \qquad (3.10)$$

Note that $\varepsilon^M_{z\phi}$ has been assumed to be constant along the gap (i.e., = an averaged value) and can be evaluated by the Eifler-Nijsing recommendation by Eqn. 3.8.b where along the gap, $\frac{r_m - R}{R}$ is obtained from VELASCO as YM.

Another definition is introduced, i.e., the "mixing distance

$$\overline{Z^{*M}_{ij}} \text{ where } \overline{Z^{*M}_{ij}} = Y_{ij}\, \overline{L^{*M}_{ij}} \qquad (3.11)$$

from 3.9 we obtain

$$\overline{Z^{*M}_{ij}} = \frac{\overline{V}_j - \overline{V}_i}{\frac{1}{R}\,\overline{\frac{1}{\xi}\frac{\partial v_z}{\partial \phi}}} \qquad (3.12)$$

Now utilizing Eqn. 3.12 in Eqn. 3.8.d we obtain:

$$\overline{W^{*M}_{ij}} = -\mu \frac{b}{R} \left(1 + \frac{\varepsilon^M_{z\phi}}{\nu}\right) \frac{R}{\overline{Z^{*M}_{ij}}} = -\mu b \left(1 + \frac{\varepsilon^M_{z\phi}}{\nu}\right) / \overline{Z^{*M}_{ij}} \qquad (3.13)$$

This last relationship corresponds to the usual definition of the turbulent mixing interchange $W'_{ij}$ [ Ref. 5]:

$$W'_{ij} = -\rho \varepsilon^M_{z\phi}\, t / Z_{ij} \qquad (3.14)$$

Finally we introduce a new definition for the mixing Stanton number,

$$M^{*M}_{ij} = \frac{\overline{W^{*M}_{ij}}}{G_i b} \qquad (3.15.a)$$

and

$$\beta^* = \frac{\overline{W^{*M}_{ij}}}{Gb} \qquad (3.15.b)$$

where $G = \frac{1}{2}(G_i + G_j)$. Equations (3.15) differ from the definition $M_{ij} = \frac{W'_{ij}}{G_i c}$ and $\beta = \frac{W'_{ij}}{Gc}$ (Eq. (5) of Ref. 7 ) only by the contribution of the molecular transport effect since $c \equiv b$.

Notes on the Peripheral and Corner Region

The major change in the formulation for the peripheral region is to use the cartesian coordinate system in a region between the wall and the zero shear stress line (A) and the cylindrical coordinate system from the zero shear stress line to the rod surface (B). The Eqns. (3.1) to (3.8) become

$$\tau_x = -(\mu + \rho \varepsilon^M_{zx}) \frac{\partial v_z}{\partial x} \qquad (3.16.a)$$

$$\tau_\phi = -(\mu + \rho \varepsilon^M_{z\phi}) \frac{1}{r} \frac{\partial v_z}{\partial \phi} \qquad (3.16.b)$$

$$\tau_{ij} = \int_A \tau_x(y)dy + \int_B \tau_\phi(r)dr \qquad (3.17)$$

$$\overline{\tau_{ij}} = \tau_{ij}/b \qquad (3.18)$$

$$\overline{\tau'_{ij}} = (b)\overline{\tau_{ij}} \qquad (3.19)$$

where for a peripheral subchannel $b \equiv \frac{PW-D}{2}$

$$\overline{W^{*M}_{ij}} = \overline{\tau'}_{ij} \,/\, (\overline{V}_j - \overline{V}_i) \qquad (3.20)$$

where A and B in Eqn. (3.17) represent the lengths over which integration is performed.

### 3.2 Numerical Consideration

To obtain $\overline{W_{ij}^{*M}}$, differentiating and integrating processes are necessary. The integration has been performed by using the Simpson $\frac{3}{8}$ rule, whereas the differentiation has been done by the following modification of the three point rule. When the mesh sizes, $\Delta\phi$ and $\Delta x_i$, are sufficiently small, the local velocity gradient $\left.\frac{\partial v_z}{\partial \phi}\right|_i$ and $\left.\frac{\partial v_z}{\partial x}\right|_i$ will be approximated by the usual finite difference approach. However every velocity distribution computation code does not always give the velocity at the necessary position for this work which is coincident with the subchannel boundary position. This is the case for VELASCO output and therefore the usual central difference approximation has been modified by giving a correction term which is a function of $\Delta$, the deviation of the subchannel boundary position from the closest peripheral position. Hence, the value of differentials at any position is given in terms of parameters at three points:

$$\frac{\partial u}{\partial \xi} = \frac{1}{2h}(u_2 - u_o) + F(\Delta, h, u_o, u_1, u_2) \qquad (3.21)$$

where F is the correction term, $\Delta$ is the deviation of subchannel boundary position, $\xi$, from the mesh position $\xi_1$, i.e.,

$$\xi - \xi_1 = \Delta \qquad (3.22.a)$$

$$\xi_1 - h = \xi_o \qquad (3.22.b)$$

$$\xi_1 + h = \xi_2 \qquad (3.22.c)$$

$$u_o = u(\xi_o) \qquad (3.22.d)$$

$$u_1 = u(\xi_1) \qquad (3.22.e)$$

$$u_2 = u(\xi_2) \qquad (3.22.f)$$

$$u = u(\xi) \qquad (3.22.g)$$

To find F, a second order Lagrangian interpolation was employed because the shape of the peripheral velocity distribution is neither rapidly increasing nor decreasing as is obvious from physical insight of the behavior of the hydraulics of the rod configurations. The result is,

$$F = \frac{\Delta}{h^2}\,(u_2 - 2u_1 + u_o) \qquad (3.23)$$

Equations (3.21 and 3.23) have truncation error of $O(h^2)$. The computer code listing for $\overline{W_{ij}^{*M}}$ is given in Appendix C.

## 3.3 Cases considered

Various bundle sizes have been investigated. The following is a list of all the cases considered (Table 1).
These types of configurations are illustrated in Figs.1 to 3 corresponding to 19, 37 and 61 pin bundles. Each subchannel boundary position and each subchannel boundary is consecutively numbered as shown in these figures. Calculations are based on a consistent arbitrarily chosen unit length and unit velocity.

The velocity gradients (grad $u = \frac{1}{r}\frac{\partial u}{\partial \phi}$) are computed by a data processing routine and its input data for a 79 pin bundle, $Re=10^5$, case 9 are attached as an example (Appendix D). Other physical quantities such as $\overline{\tau_{ij}}$, $\overline{W_{ij}^{*M}}$, $\overline{L_{ij}^{*M}}$ are easily obtained from (grad u )'s as described in section 3.4.

The sample case of [Ref. 4] for a 37 pin bundle specified 15 iterations as necessary input data. Therefore it is concluded that the results obtained here for the 19 and 37 pin bundles are satisfactory since a large number of iterations were specified (15 and 20) and but only 12 and 13 iterations were required for a convergence criterion GRENZ = .0005.

## 3.4 Calculation Procedure for Desired Parameters

3.4.1 $\overline{\text{grad u}}$-obtained directly from the data processing routine (Appendix D) which operates on VELASCO output. It appears as the parameters DVDX.

3.4.2 $\overline{Z_{ij}^{*M}}$-obtained by inverting the data processing routine output parameter ZM.

3.4.3 $\varepsilon_{z\phi}^{M}/\nu$ — The value of $\varepsilon_{\phi}^{M}$ along the subchannel boundary is obtained from VELASCO in two parts - each part taken from a pin wall to the line of zero shear stress (which is not necessarily the geometric midpoint between rods). The equations (3.8.b) and (3.13) are utilized to get numerical values.

Since there is no explicit output for $\varepsilon_{z\phi}^{M}$ in VELASCO, the equation $y_m^+ = \sqrt{\frac{\tau_R}{\rho}}(r_m - R)/\nu$ (YPM in VELASCO notation) is employed and

YPM is directly obtained by hand calculations using parameters of the VELASCO printout as follows:

YPM = WUT * RET * YM(IZ,IC)/(2.DO * DHTOT)

and

WUT = DSQRT(DABS(T(IZ,IC)))

where

RET, YM(IZ,IC), DHTOT

and

T(IZ,IC) are output values of VELASCO. See Ref. 4 for the notations.

Finally $\varepsilon_{z\phi}^{M}/\nu$ along the open gap is considered to be an arithmetic average of those of the pair boundaries (for example, in case of 19 pin rod bundle, $\varepsilon_{z\phi}^{M}$ along the boundary number 1 is an arithmetic average of $\varepsilon_{z\phi}^{M}$ of boundary positions 1 and 4).

3.4.4 $\overline{W_{ij}^{*M}}$ - This is obtained by means of Eqn. (3.13), $\overline{Z_{ij}^{*M}}$ (from 3.4.2), $\overline{\varepsilon_{z\phi}^{M}}$ (or denoted $\varepsilon_{z\phi}^{M}$ for simplicity, obtained as shown in 3.4.3) and open gap length b. The material properties are those of Na at 700°C and R = 0.25 cm. Note that b = P-D for the interior region and b = $\frac{PW-D}{2}$ for the peripheral region.

## 4. Results (without secondary flow consideration)

### 4.1 Velocity Profile

A typical example is shown in Fig. 4. Only velocities of coolant in the neighborhood of boundary number 1 and 2 of thirty-seven rod bundle (see Fig. 2) are illustrated. Subchannel bulk velocities for each case are listed in Table 3.

### 4.2 The Symmetry

The geometrical symmetries in finite triangular arrays are important factors effecting the magnitude of momentum cross flow. Significant change in velocity gradient across the boundary is observed along the corner subchannel boundary (boundary #1 of 19 pin bundle, #2 of 37 pin and 61 pin bundles), where the boundaries lose symmetry. (Figs. 5 and 6) $\overline{W_{ij}^{*M}}$ is expected to be a function of wall shear stress distribution in the same manner as is the secondary flow distribution.

### 4.3 Bundle Size

Velocity gradients for each case are shown as a function of radial extent. These gradients depend strongly on the size of the bundle especially in peripheral and corner regions. As the number of pins becomes larger, (grad u) in the central region of the bundle becomes constant and even smaller along the gap for a same Re (Fig. 5, boundaries 4,3,2 versus Fig. 6, boundaries 7, 4 , 3). This implies that we can possibly predict analogous subchannel boundaries of various sizes of triangular bundle arrays based on even smaller size bundles. See Table 4.

For example, a good analogy is made for the central region as far as the shape of $\overline{\tau_{ij}}$ is concerned (Figs. 5 and 6). It should be, however, noted that the magnitudes of $\overline{\tau_{ij}}$ differ greatly and $\overline{W_{ij}^{*M}}$'s for boundaries of a large bundle may not easily be predicted by the information obtained from a small size, i.e., 7 pins, 19 pins.

4.4 Calculated Values of $\overline{\text{grad } u}$, $\overline{Z_{ij}^{*M}}$, $\varepsilon_{z\phi}^{M}$, $\overline{W_{ij}^{*M}}$ and $\beta^{*}$

The averaged velocity gradient along the gap is almost proportional to Reynolds number at each corresponding boundary for the same type configuration (Fig. 7 and Table 5).

$1/\overline{Z_{ij}^{*M}}$ is listed in Table 6. Note that $\overline{Z_{ij}^{*M}}$ show very small values at the boundary #1 of 37 pin bundle case because $(\overline{V}_2-\overline{V}_3)$'s get as small as in the central region and the vu's are almost of the same order of the other subchannel boundaries. (See Table 5) On the other hand, at the boundary #2 of 37 pin case, although Table 5 shows vu's have very big values, $(\overline{V}_1-\overline{V}_2)$'s are much larger than at any other boundaries by the order of hundred, therefore $\overline{Z_{ij}^{*M}}$ is near the largest at the boundary #2 (i.e. $1/\overline{Z_{ij}^{*M}}$ smallest). These, however, indicate that in the corner channels, the flow is most interacted with adjacent subchannels. However the interaction between edge channels is relatively small. In general, major momentum flow is observed at the boundary of edge-central, corner-edge subchannels. The same phenomena are observed for the 19 pin bundle case. Fig. 8 and Fig. 9 illustrate the similarity at

Re $10^5$ between subchannel boundary #2 of 37 pin, case 9 and #1 of 19 pin, case 4 with respect to values of vu and $1/\overline{Z_{ij}^{*M}}$.

Galbraith and Knudsen, Rowe and Angle and other previous investigators showed that except for the relatively low Reynolds number range (< 5000), the mixing Stanton number $M_{ij}$ or $\beta$ and mixing distance $Z_{ij}$ are independent of Reynolds number, particularly at larger element spacings and higher Reynolds number (>100,000) for an ideal surface condition. And it is reported that [Ref. 8] without molecular effect, $Z_{ij}$ is predicted with good agreement to be proportional to $Re^{0.1}$ with the use of mixing parameter defined by Ingessen and Hedberg. Hence $\overline{W_{ij}^{*M}}$ is expected to be nearly proportional to Re if $\varepsilon_{z\phi}^{M}/\nu \gg 1$ (i.e., the turbulent interchange overcomes the molecular effect) and constant if $\varepsilon_{z\phi}^{M}/\nu \ll 1$ (i.e., the molecular effect is dominant to the turbulent effect - this is not the case for high Reynolds number). As is shown in Table 6 and Fig. 10 we see the weak dependency of $1/\overline{Z_{ij}^{*M}}$ on Reynolds number, which is expected by the above investigations.

The dimensionless averaged circumferential eddy diffusivity along the gap $\varepsilon_{z\phi}^{M}/\nu$ is given in Table 7 and Fig. 11. These results show the weak dependency of this parameter on position for boundaries located inside the central region (i.e., within the infinite rod array ) and on the size of the bundle.

Table 8 and Figs. 12 and 13 give the list of computed $\overline{W_{ij}^{*M}}$ along each subchannel boundary of each case.

The large discrepancy of bulk velocities in the adjacent subchannels does not necessarily mean a lot of momentum transport across the boundary. For example, see the boundary 2 of the 37 rod bundle. As a general view of the results, the larger is the bulk velocity difference, the smaller is the $\overline{W_{ij}^{*M}}$. Figs. 12 and 13 give the comparison of 19 pin bundle and 37 pin bundle cases at Re=$10^5$.

Table 8 and Fig. 14 indicate, that for both 19 and 37 pin bundles and material properties of Na at 700° C,

$$\overline{W_{ij}^{*M}} = K \times Re^{0.926}$$

where K is a constant and has different values for each boundary position and size of the bundle. For instance, for a 19 pin bundle,

$K = 4.55 \times 10^{-5}$ for boundary #1

$2.46 \times 10^{-4}$ for boundary #2

$5.37 \times 10^{-4}$ for boundary #3

$4.80 \times 10^{-4}$ for boundary #4

The mixing Stanton number is defined by Eqns. 3.15.a or 3.15.b i.e.,

$$\beta^{*} = \frac{\overline{W_{ij}^{*M}}}{Gb} \qquad (3.15.b)$$

In this paper, G and b are treated as following:

$$G = \frac{1}{2}(G_i + G_j)$$
$$= \rho \times (\bar{V}_i + \bar{V}_j)/2$$

and

$$b = P-D \quad \text{for central region}$$

$$= (PW-D)/2 \quad \text{for peripheral region}$$

and $\beta^*$'s are computed as

$$\beta^* = \frac{1}{P} \times \frac{\overline{W_{ij}^{*M}}}{\frac{(V_i + V_j)}{2} \times b}$$

For all boundaries of 19 pin cases, $\beta^*$'s are calculated and given in Table 9 and Fig. 15. For the relatively small size 19 pin bundle examined, $\beta^*$'s were not constant with Re but weak and well behaved functions of Re.

## 4.5 Secondary Flow

So far the secondary flow effect has been neglected and the attention was focussed on the velocity gradient along the subchannel boundaries and its averaged value, which involves turbulent and molecular exchange. Recently, however, the importance of secondary flow effect has been noted and inevitably this effect should be considered in the ordinary thermal hydraulic design aspect. The work done in this paper enables us to take into account this effect easily when an existing subchannel analysis code is to be used. One can calculate the magnitude of secondary flow transport of energy and/or momentum as following and can use it suitably as an input to $\overline{W_{ij}^{*E}}$ and $\overline{W_{ij}^{*M}}$ depending upon assumptions of the original distributed parameter code and lumped parameter code. A shear stress with secondary flow considerations is directly proportional to

$$\frac{1}{r}\frac{\partial v_z}{\partial \phi} + \frac{1}{\nu + \varepsilon_\phi^M} v_z v_\phi$$

with the same proportionality constant as the case without secondary flow. It should be noted that for consistency, use of $\varepsilon_{z\phi}^{M} = 0.154\, y_o(\tau_w/\rho)^{1/2}$ for the momentum eddy diffusivity expression is required as long as VELASCO code is employed. Calculations of $\overline{\tau_{ij}}$ for the 37 pin bundle were made with an assumed secondary flow having the following characteristics.

$$V_{sec} = 1.146 * \frac{Pe_{sec}}{Pe} * \frac{d\sqrt{\frac{\tau_R}{\rho}}}{dx} * \cos(\pi\tau)$$

where $Pe_{sec}$ is the peripheral extent along the wall of a closed secondary flow vortex. By definition it is equal to the distance between two adjacent extreme values of the wall shear stress curve. The results obtained were a 12% increase in $\overline{\tau_{ij}}$ along the edge subchannel boundary (i.e., boundary #1 of 37 pin case), a 5% increase along the corner subchannel boundary (boundary #2). In the central region, however, because of degree of symmetry, the secondary flows apparently do not cause significant changes in velocity gradients at subchannel boundaries because negligible changes in $\overline{\tau_{ij}}$ were noted. Hence the secondary flow is not of great importance to the transport pehnomena between interior subchannels.

## 5. Recommended Use of Results

Application of subchannel analysis codes like COBRA involves separate consideration of intersubchannel transport due to natural mixing effects (i.e., molecular diffusion, diversion cross flow and turbulent diffusion) and other forced cross flow mixing.

The COBRA code formulates the contributions due to turbulent interchange and thermal conduction separately as

$$(h_i - h_j)\frac{W'_{ij}}{m_i} - (T_i - T_j)\frac{C_{ij}}{m_i} \qquad \text{(Ref. 2, Eqn. 2)}$$

COBRA presents several correlation forms for $W'_{ij}$ (called $W'_k$ where K is a subchannel connection number between i and j) the most sophisticated being

$$W'_K = a\, Re^b \frac{S_K}{Z_K} \overline{D}\, \overline{G} \qquad \text{(Ref. 2, Eqn. C-23)}$$

and one general form for the conduction coefficient

$$C_K = \left(\frac{k_i(K) + k_j(K)}{2}\right) \frac{S_K}{Z_K}\, Kg \qquad \text{(Ref. 2, Eqn. C-28)}$$

The value of $Z_K$ to be used in the above equations can be selected by the user. Properly it should be that effective mixing distance where

$$Z_{ij} \equiv \frac{\overline{T}_j - \overline{T}_i}{\frac{1}{\xi}\frac{\partial T}{\partial \phi}}$$

$Z_{ij}$ selected as above is that distance which when used with subchannel average temperatures produces a gradient, $\frac{\overline{T}_j - \overline{T}_i}{Z_{ij}}$ which equals the true gap gradient. Note carefully that the approach usually adopted for simplicity is to take $Z_{ij}$ as the centroid to centroid distance between subchannels (Ref. 2, page c-5). If this is done, then the burden of producing valid correlations is shifted to Eqn. C-23 and it is required that the correlation for $W'_k$ be formulated to work in the integral sense.

The formulations in this paper are in momentum exchange terms only because VELASCO presently performs a momentum and not an energy solution. Therefore the spatially varying exchange coefficients developed here, $\overline{W^{*M}_{ij}}$, are not analogous to the Cobra terms $W'_K$. Rather the term $\overline{W^{*E}_{ij}}$ derivable by our methods from a "thermal" VELASCO would be analogous to $W'_K$.

The final result for $\overline{W_{ij}^{*E}}$ is given as analogous to results of Table 8, and these values would be recommended for input values of $W'_k$. Note that use of these recommended values will result in separate $W'_k$ input values for each boundary. Functional dependency of $\overline{W_{ij}^{*E}}$ on Reynolds number would be developed analogous to Section 4.4 yielding a value of b where $\overline{W_{ij}^{*E}} = W'_k = K\ Re^b$. This result can be used to interpolate or extrapolate Table 8 type values for varying Reynolds numbers in the turbulent regieme.

## References


1. H. Ramm, K. Johannsen and N.E. Todreas, "Single Phase Transport within Bare Rod Arrays at Laminar, Transition and Turbulent Flow Conditions," Nuclear Engineering and Design, Vol. 30 (1974) No. 2, pp. 186-204.

2. D.S. Rowe, "COBRA IIIC: A Digital Computer Program for Steady State and Transient Thermal-Hydraulic Analysis of Rod Bundle Nuclear Fuel Elements," Battelle Pacific Northwest Lab., March 1973.

3. R.W. Bowring, "HAMBRO - A Computer Program for the Subchannel Analysis of the Hydraulic and Burnout Characteristics of Rod Clusters," (Part I), "General Description, AEEW-R524, U.K. Atomic Energy Authority, Winfrith (1967).

4. W. Eifler and R. Nijsing, "VELASCO - Velocity Field in Asymmetric Rod Configurations," ISPRA Report.

5. J.T. Rogers and R.G. Rosehart, "Mixing by Turbulent Interchange in Fuel Bundles, Correlations and Inferences," ASME 72-HT-53.

6. R. Nijsing and R. Eifler, "Axial Development of Temperature Fields in Hexagonal Fast Reactor Fuel Rod Assemblies with Liquid Metal Cooling," paper 60 Karlsruhe Meeting, October 1973.

7. J.T. Rogers and N.E. Todreas, "Coolant Interchannel Mixing in Reactor Fuel Rod Bundles, Single-Phase Coolant," Heat Transfer in Rod Bundles, ASME, N.Y. 1968.

8. L. Ingerson and S. Hedberg, "Heat Transfer Between Subchannels in a Rod Bundle," Paper EC7, 11, 4th International Heat Transfer Conference, Paris (Sept. 1970).

TABLE 1

| Case No. | No. of Pins | Re | Type of configuration | P/D | PW/D |
|---|---|---|---|---|---|
| 1 | 19 | $0.1 \times 10^5$ | Triangular bare rod array | 1.25 | 1.15 |
| 2 | 19 | 0.25 | " " " " | " | " |
| 3 | 19 | 0.5 | " " " " | " | " |
| 4 | 19 | 1.0 | " " " " | " | " |
| 5 | 19 | 10.0 | " " " " | " | " |
| 6 | 37 | 0.1 | " " " " | " | " |
| 7 | 37 | 0.25 | " " " " | " | " |
| 8 | 37 | 0.5 | " " " " | " | " |
| 9 | 37 | 1,0 | " " " " | " | " |
| 10 | 37 | 10.0 | " " " " | " | " |

TABLE 2

Approximate Job Run Time

| Type of Bundle | Sec/Iteration | Total Iterations to a Convergence | Number of Specified Iterations |
|---|---|---|---|
| 19 pin | ~ 3.3 sec | 12 | ~ 15 |
| 37 pin | ~ 7.0 sec | 13 | ~ 20 |
| 61 pin | ~11.5 sec | | ~52 |
| 91 pin | ~18.0 sec | | |

TABLE 3

DIMENSIONLESS SUBCHANNEL BULK VELOCITY $V_i = UB_i/UB(TOT)$
(UB(TOT) is overall channel bulk velocity of each case)

19 Pins

| Subchannel Number | Re x $10^{-5}$ 0.1 | 0.25 | 0.5 | 1.0 | 10.0 |
|---|---|---|---|---|---|
| 1 | 0.707 | 0.723 | 0.732 | 0.738 | 0.756 |
| 2 | 0.958 | 0.961 | 0.963 | 0.964 | 0.965 |
| 3 | 1.062 | 1.059 | 1.057 | 1.055 | 1.052 |
| 4 | 1.069 | 1.064 | 1.062 | 1.061 | 1.057 |
| 5 | 1.070 | 1.065 | 1.063 | 1.062 | 1.059 |

37 Pins

| Subchannel number | Re x $10^{-5}$ 0.1 | 0.25 | 0.5 | 1.0 | 10.0 |
|---|---|---|---|---|---|
| 1 | 0.689 | 0.707 | 0.716 | 0.723 | 0.741 |
| 2 | 0.938 | 0.943 | 0.945 | 0.947 | 0.949 |
| 3 | 0.943 | 0.947 | 0.949 | 0.951 | 0.953 |
| 4 | 1.040 | 1.038 | 1.037 | 1.036 | 1.033 |
| 5 | 1.042 | 1.039 | 1.038 | 1.037 | 1.034 |
| 6 | 1.046 | 1.043 | 1.041 | 1.040 | 1.038 |
| 7 | 1.047 | 1.044 | 1.043 | 1.042 | 1.040 |
| 8 | 1.048 | 1.044 | 1.043 | 1.042 | 1.040 |
| 9 | 1.048 | 1.044 | 1.043 | 1.042 | 1.040 |

TABLE 4

CORRESPONDING SUBCHANNEL BOUNDARY POSITIONS OF DIFFERENT BUNDLE SIZES

| 19 PINS | 37 PINS | 61 PINS |
|---|---|---|
| 4 | 7 | 8 |
| 3 | 4 | 6 |
| 2 | 3 | 5 |
| 1 | 2 | 2 |

TABLE 5

AVERAGED RELATIVE VELOCITY GRADIENT $\overline{\nabla u}$

ALONG THE SUBCHANNEL BOUNDARY

( u;normalized by the bundle average velocities UB(TOT) )

| 19 Pins Boundary Number | Re x $10^{-5}$ 0.1 | 0.25 | 0.5 | 1.0 | 10.0 |
|---|---|---|---|---|---|
| 1 | .310E-1 | .806E-1 | .163 | .328 | .331E 1 |
| 2 | .164E-1 | .377E-1 | .732E-1 | .145 | .146E 1 |
| 3 | .198E-2 | .432E-2 | .836E-2 | .167E-1 | .183 |
| 4 | .477E-3 | .102E-2 | .198E-2 | .400E-2 | .470E-1 |

| 37 Pins Boundary Number | Re x $10^{-5}$ 0.1 | 0.25 | 0.5 | 1.0 | 10.0 |
|---|---|---|---|---|---|
| 1 | .337E-2 | .812E-2 | .171E-1 | .354E-1 | .360 |
| 2 | .356E-1 | .811E-1 | .165 | .336 | .342E 1 |
| 3 | .161E-1 | .370E-1 | .715E-1 | .141 | .143E 1 |
| 4 | .201E-2 | .433E-2 | .832E-2 | .165E-1 | .182 |
| 5 | .153E-2 | .344E-2 | .672E-2 | .135E-1 | .148 |
| 6 | .129E-2 | .300E-1 | .586E-1 | .116 | .119E 1 |
| 7 | .434E-3 | .914E-3 | .177E-2 | .358E-2 | .424E-1 |
| 8 | .530E-4 | .954E-4 | .187E-3 | .382E-3 | .487E-2 |
| 9 | .251E-4 | .422E-4 | .828E-4 | .172E-3 | .176E-2 |

TABLE 6

INVERSE OF THE MIXING DISTANCE $1/\overline{Z_{ij}^{*M}}$ ( 1/cm )

( rod diameter D = 0.5 cm )

| 19 Pins Boundary Number | Re x $10^{-5}$ 0.1 | 0.25 | 0.5 | 1.0 | 10.0 |
|---|---|---|---|---|---|
| 1 | .123E 1 | .135E 1 | .140E 1 | .146E 1 | .158E 1 |
| 2 | .157E 1 | .155E 1 | .156E 1 | .158E 1 | .169E 1 |
| 3 | .314E 1 | .313E 1 | .315E 1 | .318E 1 | .332E 1 |
| 4 | .387E 1 | .383E 1 | .376E 1 | .371E 1 | .353E 1 |

| 37 Pins Boundary Number | Re x $10^{-5}$ 0.1 | 0.25 | 0.5 | 1.0 | 10.0 |
|---|---|---|---|---|---|
| 1 | .787E 1 | .762E 1 | .866E 1 | .918E 1 | .890E 1 |
| 2 | .142E 1 | .137E 1 | .144E 1 | .150E 1 | .165E 1 |
| 3 | .158E 1 | .156E 1 | .157E 1 | .159E 1 | .170E 1 |
| 4 | .362E 1 | .352E 1 | .349E 1 | .348E 1 | .347E 1 |
| 5 | .372E 1 | .362E 1 | .360E 1 | .362E 1 | .367E 1 |
| 6 | .132E 1 | .131E 1 | .133E 1 | .135E 1 | .147E 1 |
| 7 | .318E 1 | .307E 1 | .311E 1 | .312E 1 | .318E 1 |
| 8 | .950 | .954 | .101E 1 | .109E 1 | .157E 1 |
| 9 | .110 | .939 | .104E 1 | .123E 1 | .220E 1 |

TABLE 7

CIRCUMFERENTIAL EDDY DIFFUSIVITY $\overline{\varepsilon^{M}_{z\phi}}/\nu$
(dimensionless)

| 19 Pins Boundary Number | Re x $10^{-5}$ 0.1 | 0.25 | 0.5 | 1.0 | 10.0 |
|---|---|---|---|---|---|
| 1 | .996E 2 | .218E 2 | .398E 2 | .736E 2 | .597E 3 |
| 2 | .203E 2 | .446E 2 | .819E 2 | .151E 3 | .121E 4 |
| 3 | .205E 2 | .452E 2 | .829E 2 | .153E 3 | .123E 4 |
| 4 | .205E 2 | .452E 2 | .830E 2 | .154E 3 | .123E 4 |

| 37 Pins Boundary Number | Re x $10^{-5}$ 0.1 | 0.25 | 0.5 | 1.0 | 10.0 |
|---|---|---|---|---|---|
| 1 | .983E 1 | .215E 2 | .394E 2 | .726E 2 | .585E 3 |
| 2 | .942E 1 | .205E 2 | .376E 2 | .694E 2 | .563E 3 |
| 3 | .193E 2 | .423E 2 | .779E 2 | .144E 3 | .115E 4 |
| 4 | .195E 2 | .430E 2 | .790E 2 | .146E 3 | .117E 4 |
| 5 | .196E 2 | .430E 2 | .789E 2 | .146E 3 | .117E 4 |
| 6 | .193E 2 | .425E 2 | .789E 2 | .144E 3 | .116E 4 |
| 7 | .196E 2 | .430E 2 | .790E 2 | .146E 3 | .117E 4 |
| 8 | .196E 2 | .430E 2 | .791E 2 | .146E 3 | .117E 4 |
| 9 | .196E 2 | .430E 2 | .791E 2 | .146E 3 | .117E 4 |

TABLE 8

MOMENTUM EXCHANGE COEFFICIENT $\overline{W_{ij}^{*M}}$ ( g/sec-cm )

Case: Na coolant at 700°C

| 19 Pins Boundary Number | Re x $10^{-5}$ 0.1 | 0.25 | 0.5 | 1.0 | 10.0 |
|---|---|---|---|---|---|
| 1 | .217 | .497 | .923 | .175E 1 | .153E 2 |
| 2 | .922 | .195E 1 | .357E 1 | .663E 1 | .563E 2 |
| 3 | .186E 1 | .399E 1 | .729E 1 | .135E 2 | .113E 3 |
| 4 | .115E 1 | .244E 1 | .436E 1 | .793E 1 | .600E 2 |

| 37 Pins Boundary Number | Re x $10^{-5}$ 0.1 | 0.25 | 0.5 | 1.0 | 10.0 |
|---|---|---|---|---|---|
| 1 | .957 | .215E 1 | .438E 1 | .847E 1 | .653E 2 |
| 2 | .214 | .439 | .846 | .123E 1 | .108E 2 |
| 3 | .683 | .145E 1 | .266E 1 | .495E 1 | .420E 2 |
| 4 | .161E 1 | .333E 1 | .599E 1 | .110E 2 | .873E 2 |
| 5 | .164E 1 | .342E 1 | .619E 1 | .113E 2 | .922E 2 |
| 6 | .293 | .613 | .114E 1 | .214E 1 | .183E 2 |
| 7 | .141E 1 | .290E 1 | .534E 1 | .984E 1 | .801E 2 |
| 8 | .421 | .901 | .174E 1 | .345E 1 | .395E 2 |
| 9 | .244 | .444 | .891 | .194E 1 | .277E 2 |

TABLE 9

RELATIVE MIXING STANTON NUMBER ß*( Na coolant at 700°C )

| 19 Pins Boundary Number | Re x $10^{-5}$ 0.1 | 0.25 | 0.5 | 1.0 | 10.0 |
|---|---|---|---|---|---|
| 1 | .373E 2 | .337E 2 | .311E 2 | .293E 2 | .253E 2 |
| 2 | .761E 2 | .644E 2 | .589E 2 | .547E 2 | .466E 2 |
| 3 | .146E 3 | .125E 3 | .115E 3 | .106E 3 | .891E 2 |
| 4 | .179E 3 | .153E 3 | .137E 3 | .125E 3 | .945E 2 |

| 37 Pins Boundary Number | Re x $10^{-5}$ 0.1 | 0.25 | 0.5 | 1.0 | 10.0 |
|---|---|---|---|---|---|
| 1 | .145E 3 | .130E 3 | .132E 3 | .128E 3 | .981E 2 |
| 2 | .439E 2 | .327E 2 | .239E 2 | .226E 2 | .197E 2 |
| 3 | .572E 2 | .488E 2 | .447E 2 | .416E 2 | .353E 2 |
| 4 | .129E 3 | .107E 3 | .961E 2 | .881E 2 | .702E 2 |
| 5 | .132E 3 | .110E 3 | .992E 2 | .904E 2 | .742E 2 |
| 6 | .491E 2 | .412E 2 | .382E 2 | .358E 2 | .307E 2 |
| 7 | .112E 3 | .927E 2 | .855E 2 | .788E 2 | .643E 2 |
| 8 | .336E 2 | .288E 2 | .277E 2 | .276E 2 | .317E 2 |
| 9 | .387E 2 | .287E 2 | .285E 2 | .311E 2 | .444E 2 |

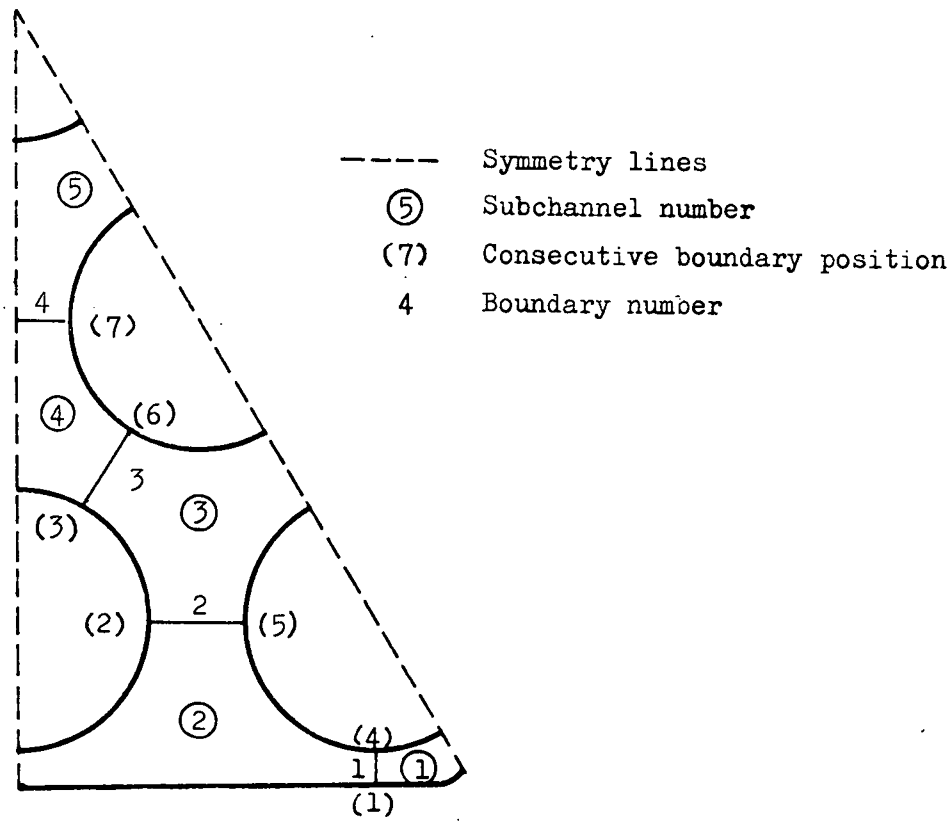


Fig. 1 Subchannels in a subarray representative for a nineteen rod array.

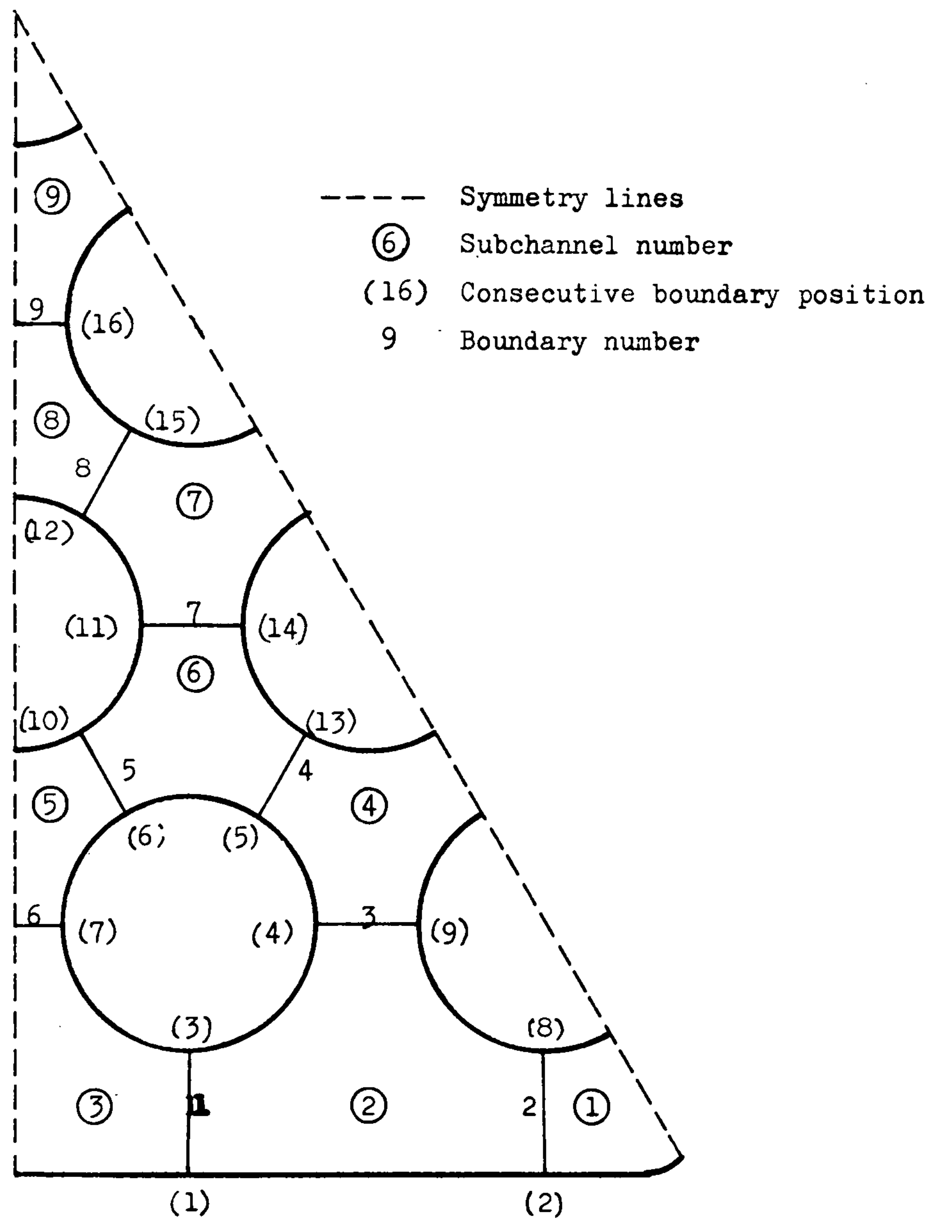


Fig. 2 Subchannels in a subarray representative for a thirty seven rod array.

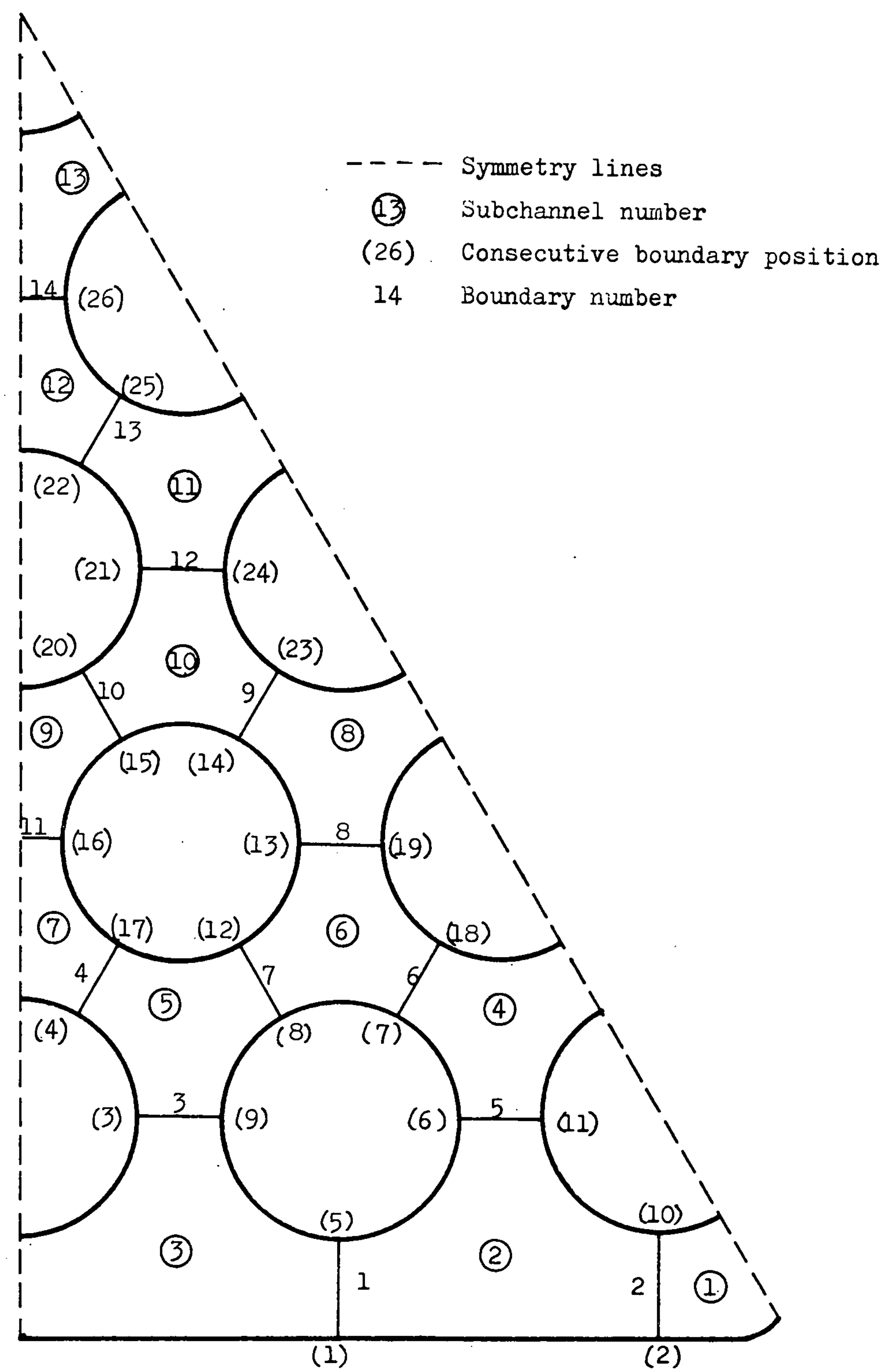


Fig. 3 Subchannels in a subarray representative for a sixty one rod array.

$$\frac{U}{UB(TOT)} = u$$

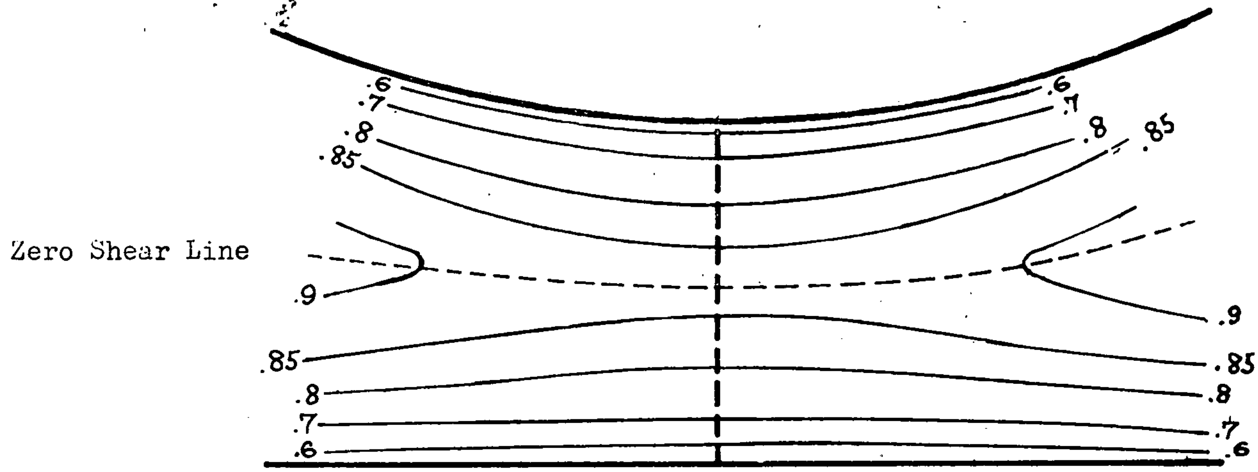


Boundary #1

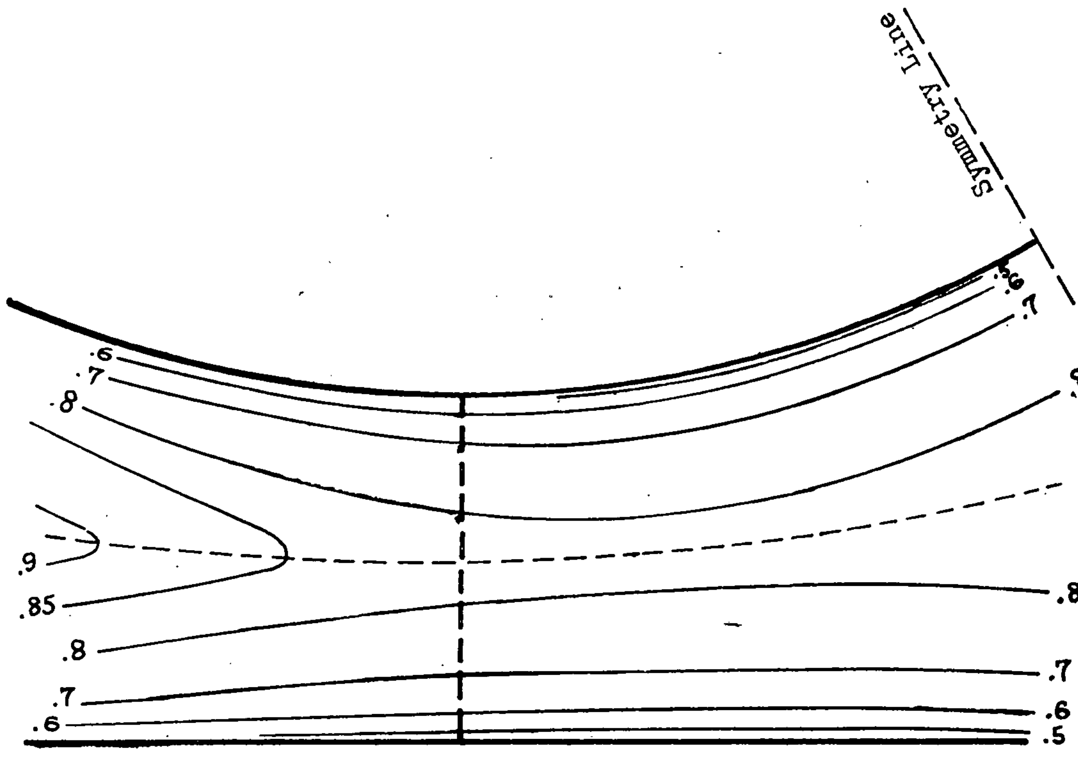


Boundary #2

Fig. 4 Velocity profile in the neighbourhood of the subchannel boundary #1 and #2 of the thirty seven pin bundle. Case 8 ( $Re = 10^5$ ).

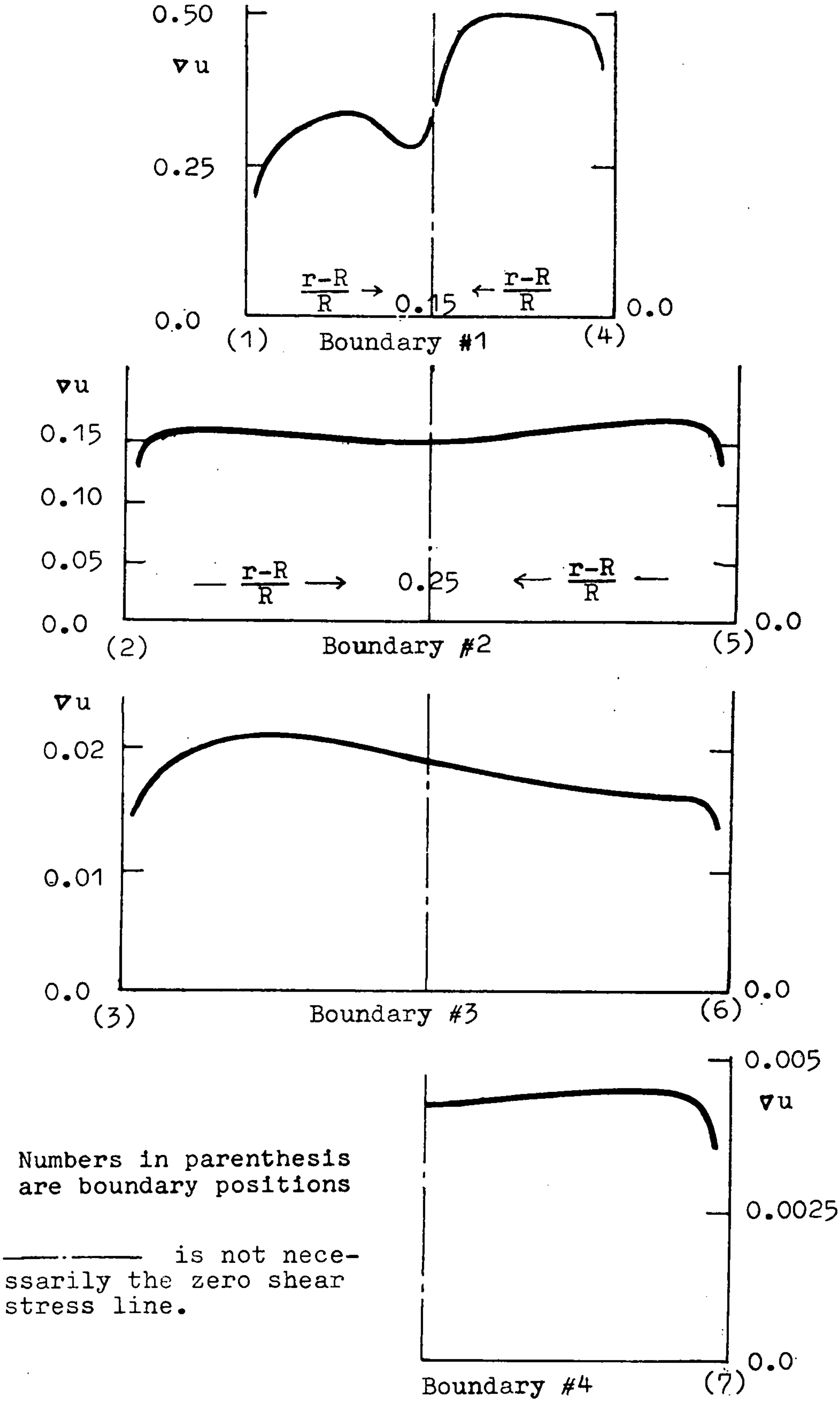


Fig. 5 Relative velocity gradient, ∇u (1/cm) along subchannel boundaries for case #4 (19 pins, Re=$10^5$)

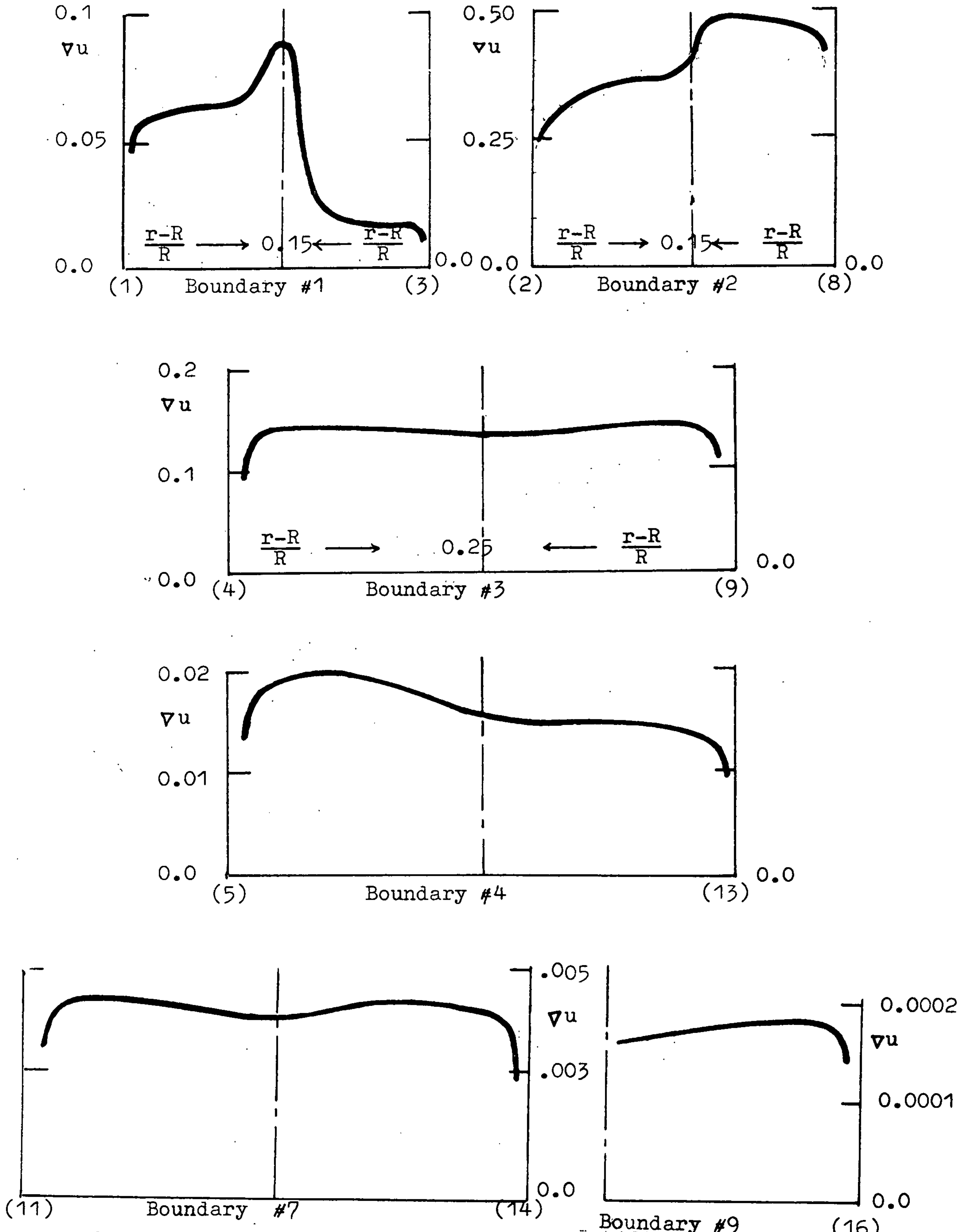


FIG. 6. Relative velocity gradient, ∇u (1/cm), along the subchannel boundaries for case #9 (37 pins, Re = $10^5$)

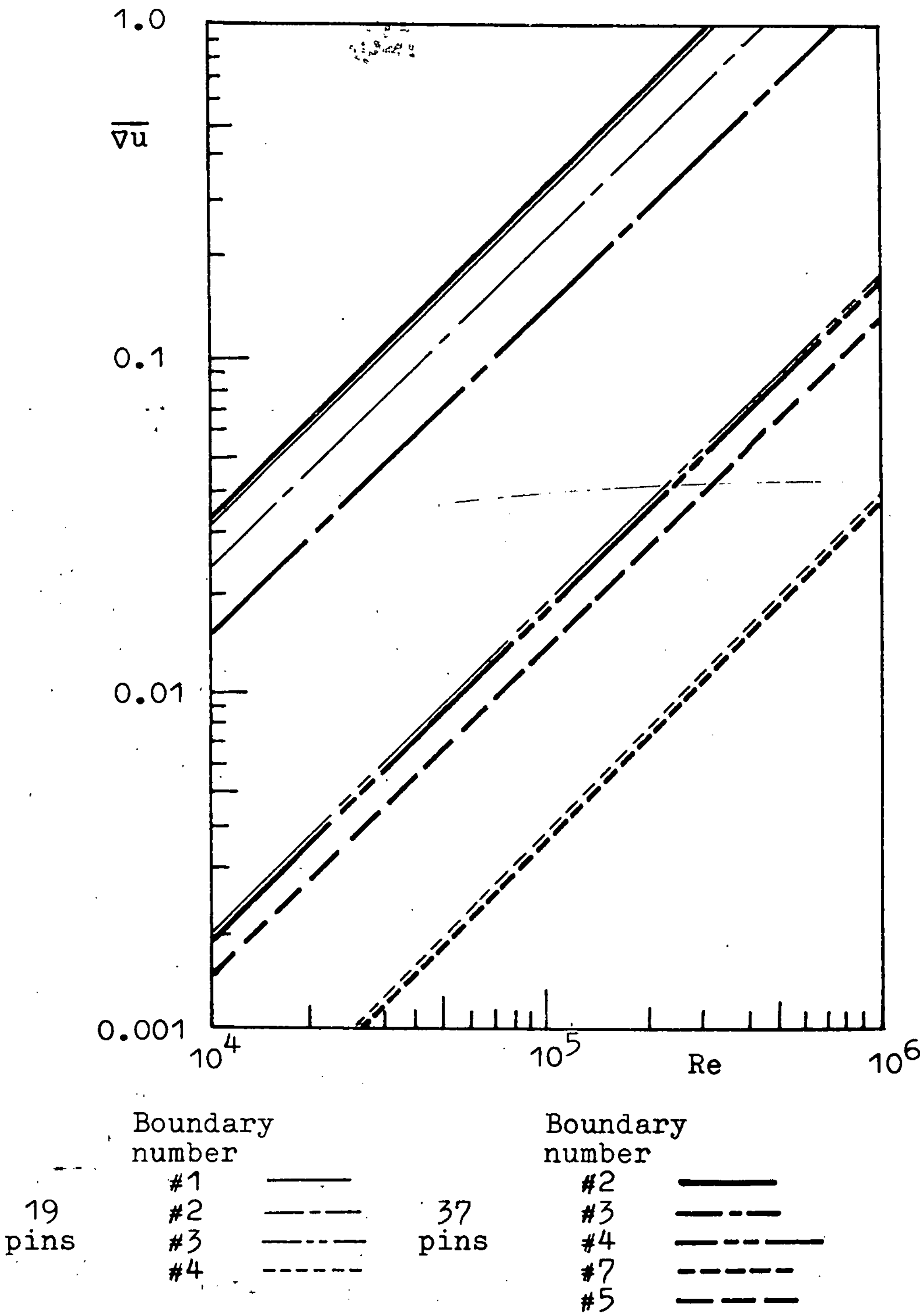


Fig. 7 Averaged relative velocity gradient along the boundary $\overline{\nabla u}$ vs. Re at each subchannel boundary of nineteen and thirty seven rod bundles.

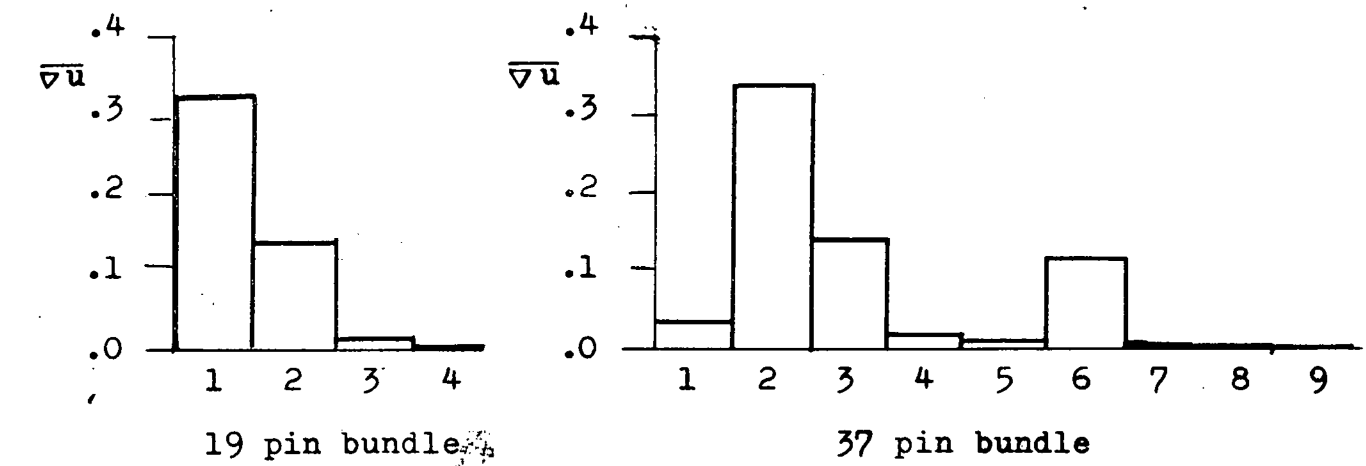


Fig. 8 Averaged relative velocity gradient ( $\overline{\nabla u}$ ) vs. subchannel boundary number; Re=$10^5$.

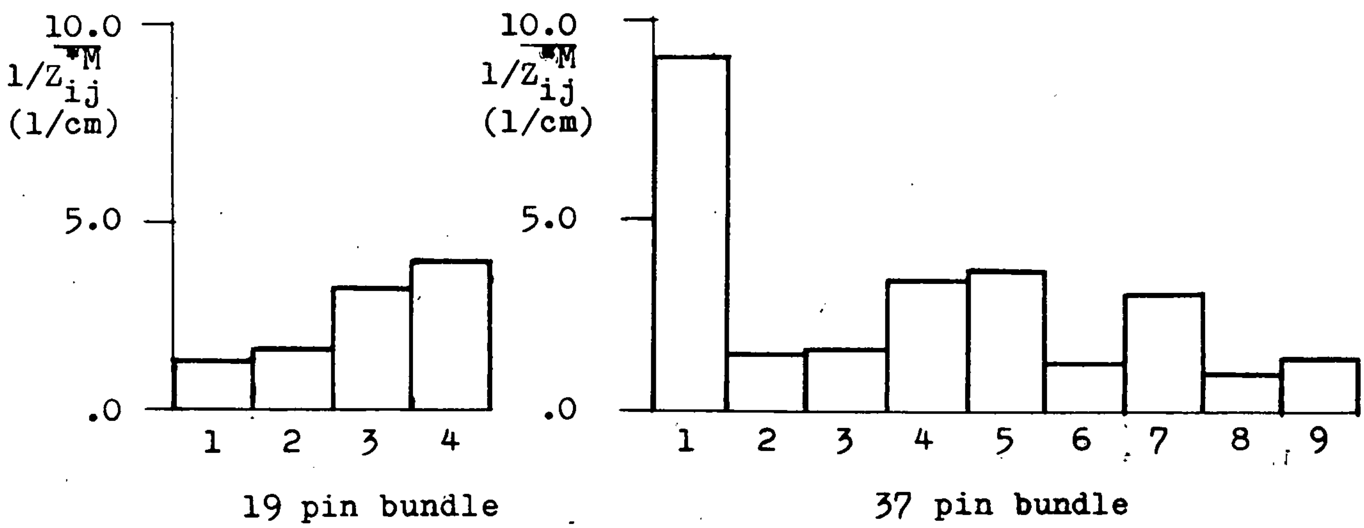


Fig. 9 Inverse of the mixing distance vs. subchannel boundary number; Re=$10^5$, rod radius=.25 cm P/D=1.25 and PW/D=1.15

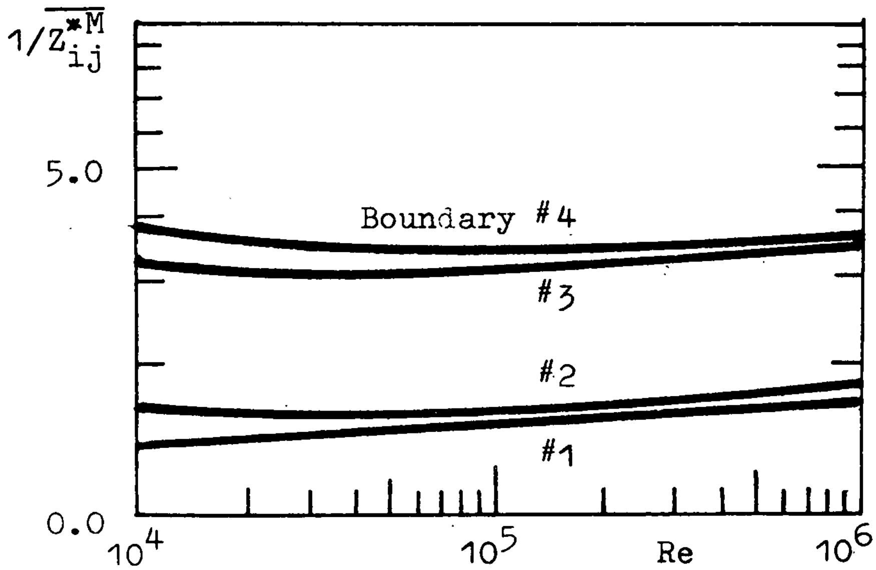


Fig. 10 Inverse of the mixing distance $1/\overline{Z^{*M}_{ij}}$ vs. Reynolds number for nineteen rod bundle. Rod radius=.25 cm, P/D=1.25 and PW/D=1.15.

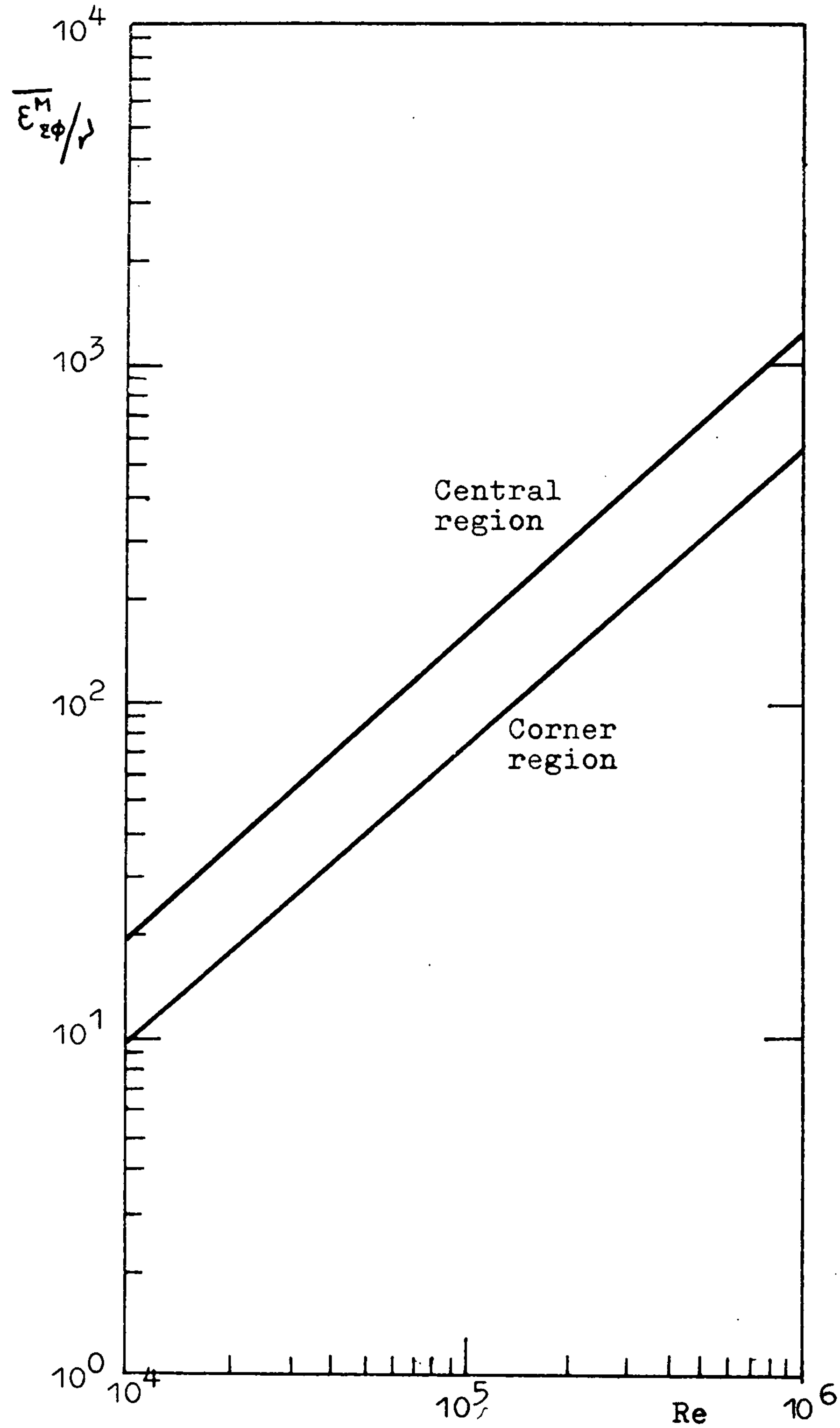


Fig.11 Circumferential eddy diffusivity in dimensionless $\overline{\varepsilon^M_{z\phi}}/\nu$ for nineteen and thirty-seven rod bundles, rod radius = .25 cm, P/D = 1.25.

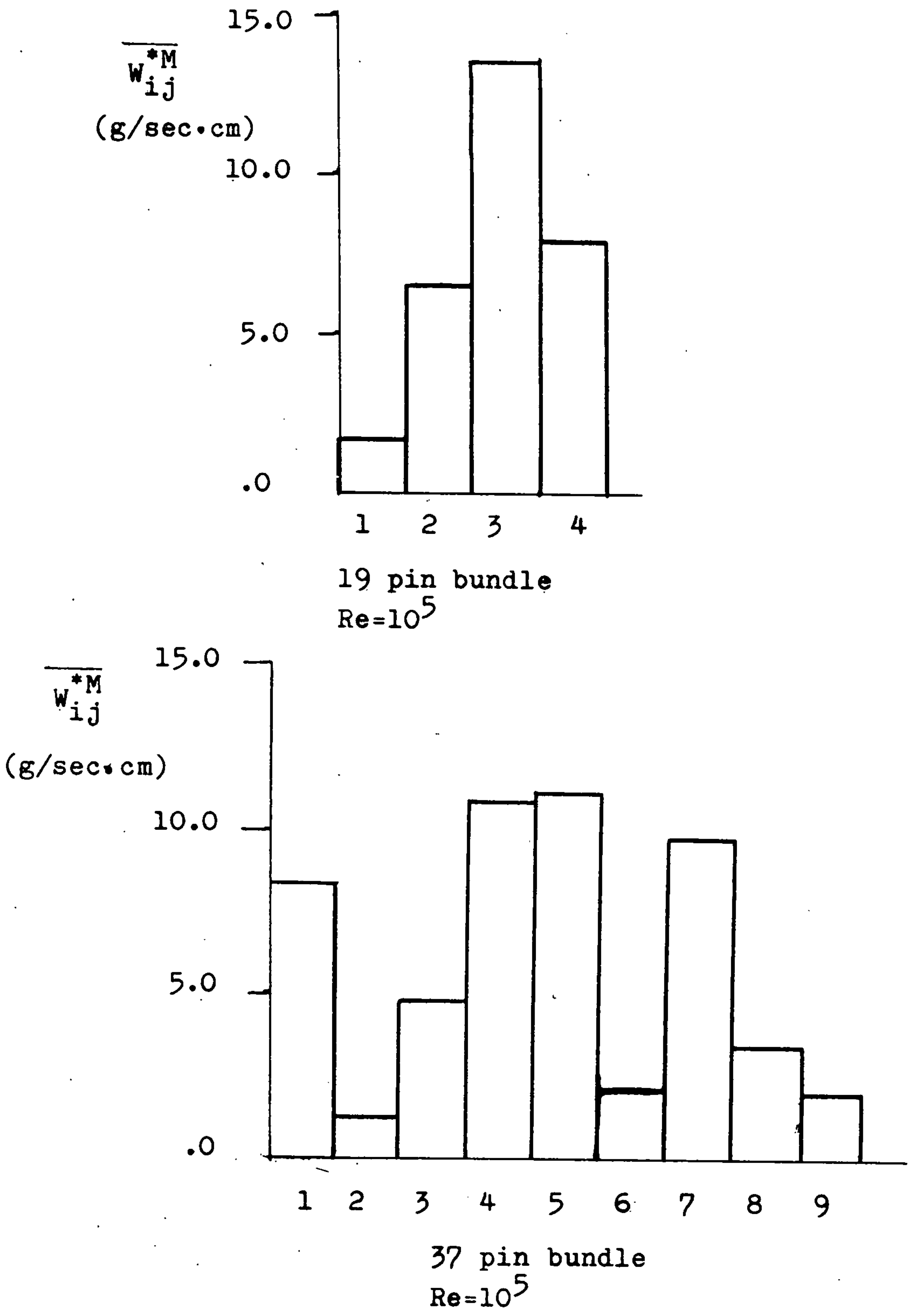


Fig.12 Momentum exchange coefficients vs. subchannel boundary number. Na coolant at 700°C, rod radius=.25 cm, P/D=1.25 and PW/D=1.15.

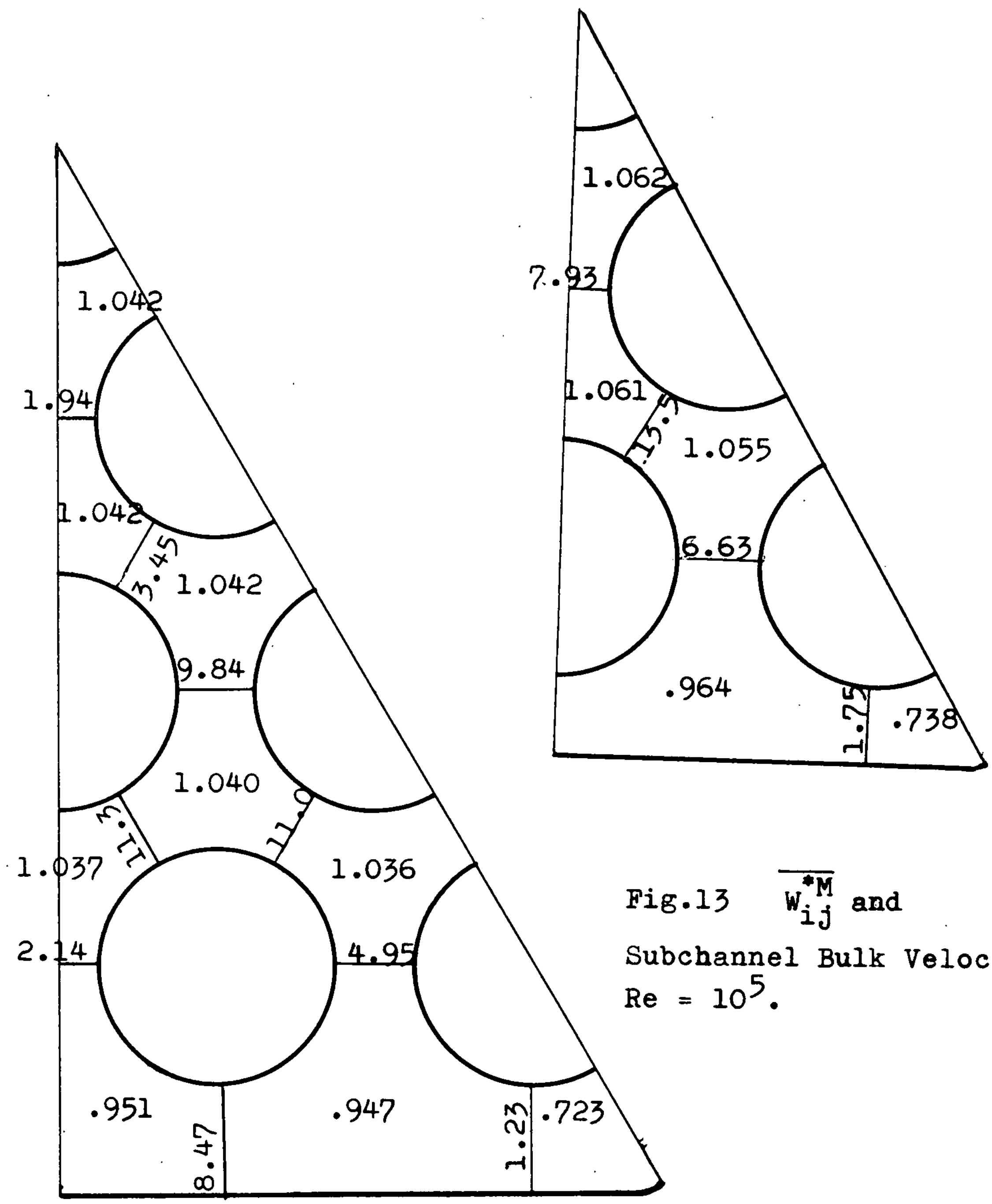


Fig.13 $\overline{W_{ij}^{*M}}$ and Subchannel Bulk Velocities. Re = $10^5$.

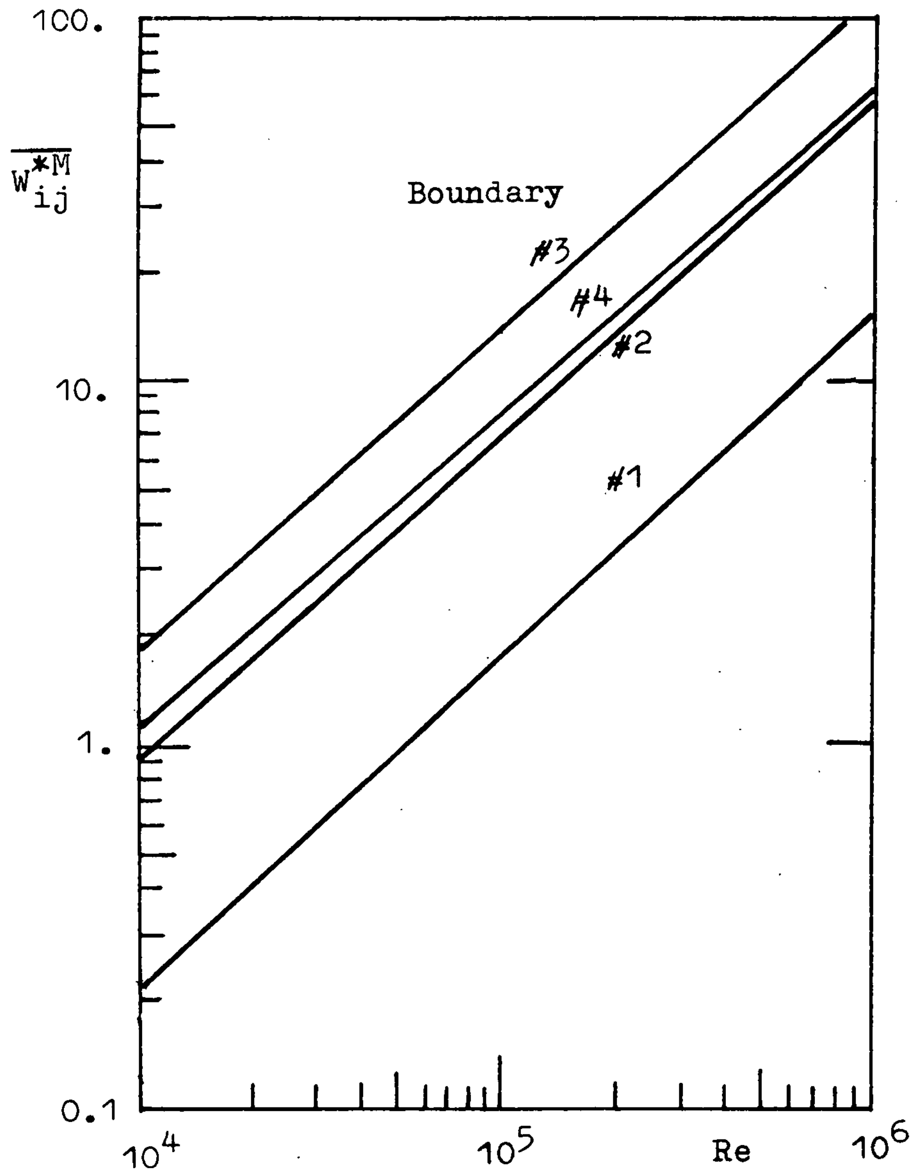


Fig. 14-1 $\overline{W_{ij}^{*M}}$ vs. Re for a nineteen rod bundle.

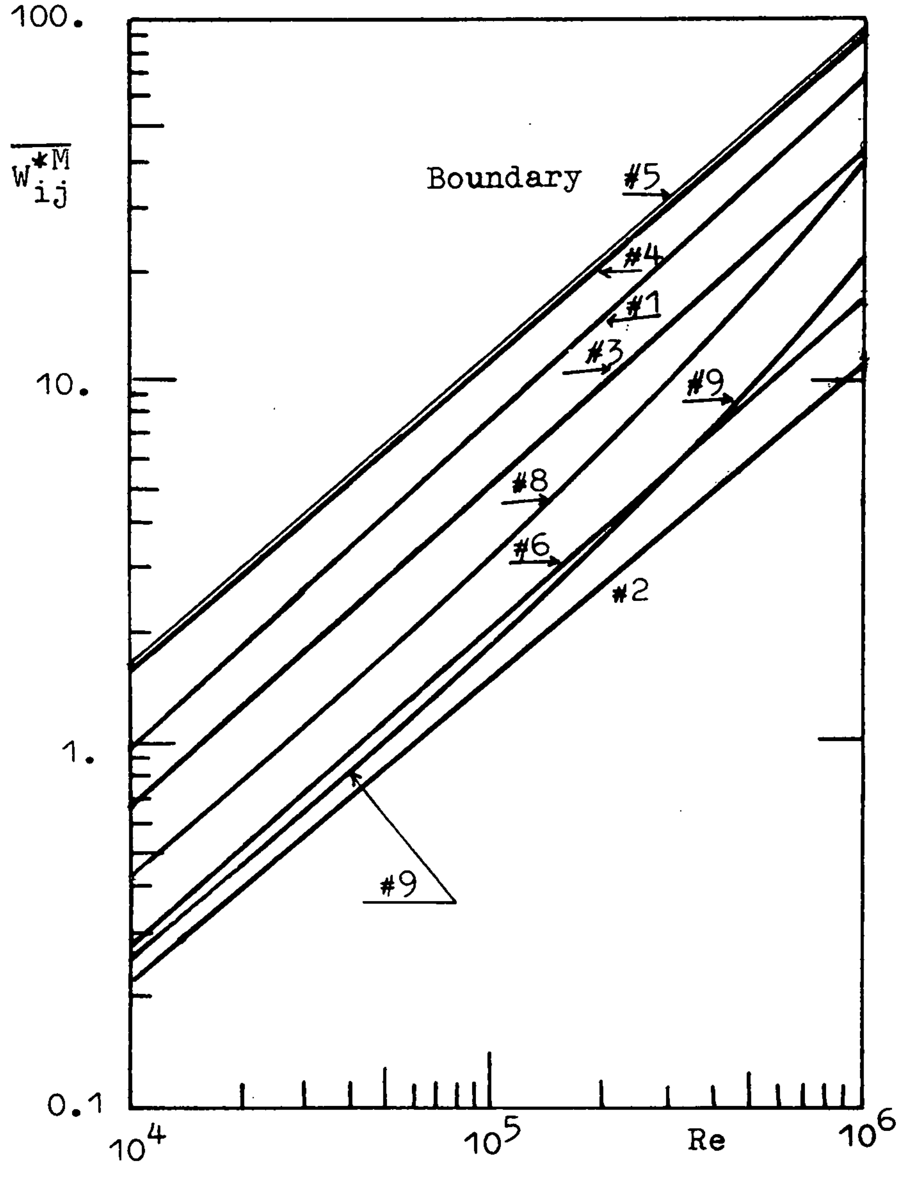


Fig. 14-2 $\overline{W^{*M}_{ij}}$ vs. Re for a thirty seven rod bundle.

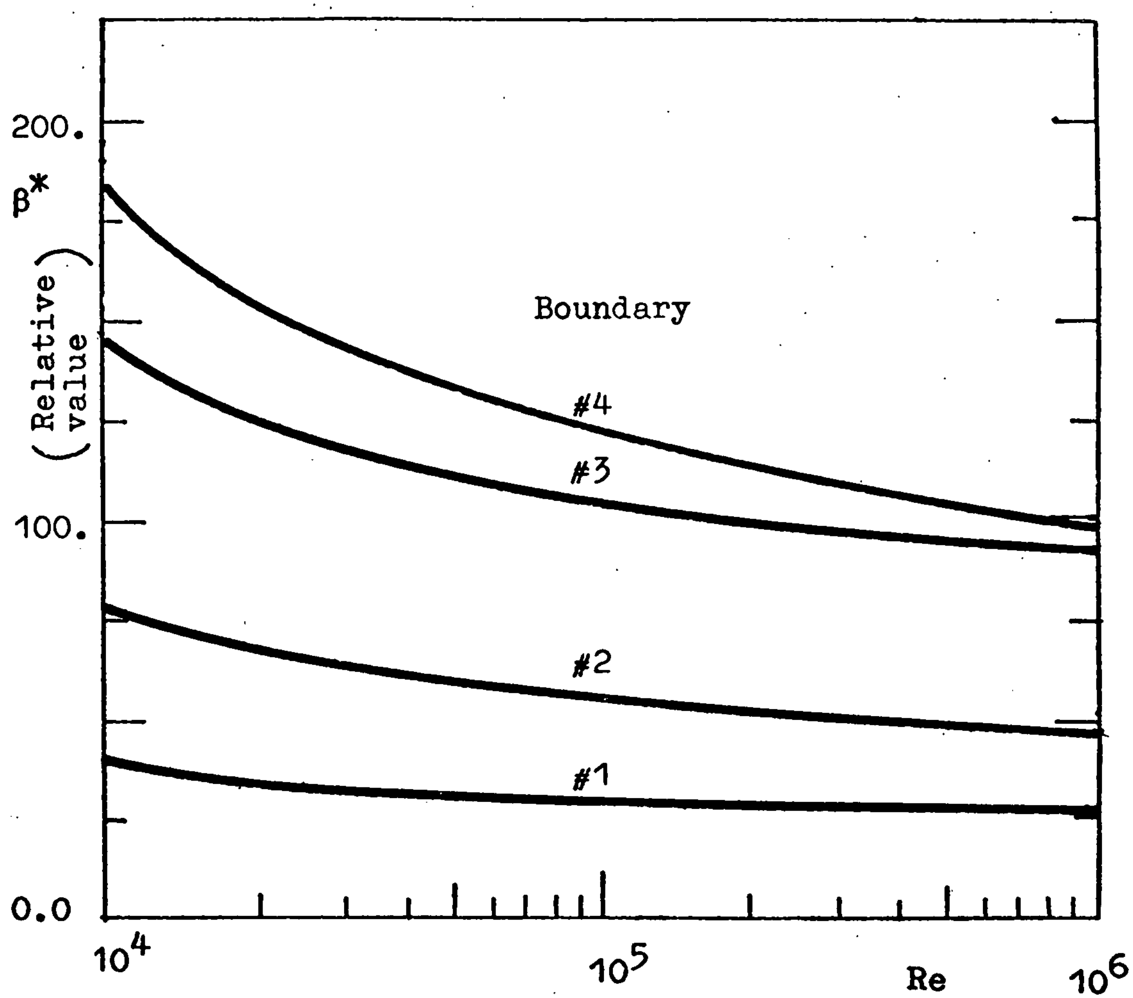


Fig.15-1 Mixing Stanton number $\beta^*$ vs. Re for nineteen pin bundle, Na coolant at 700°C, rod radius = .25 cm, P/D = 1.25.

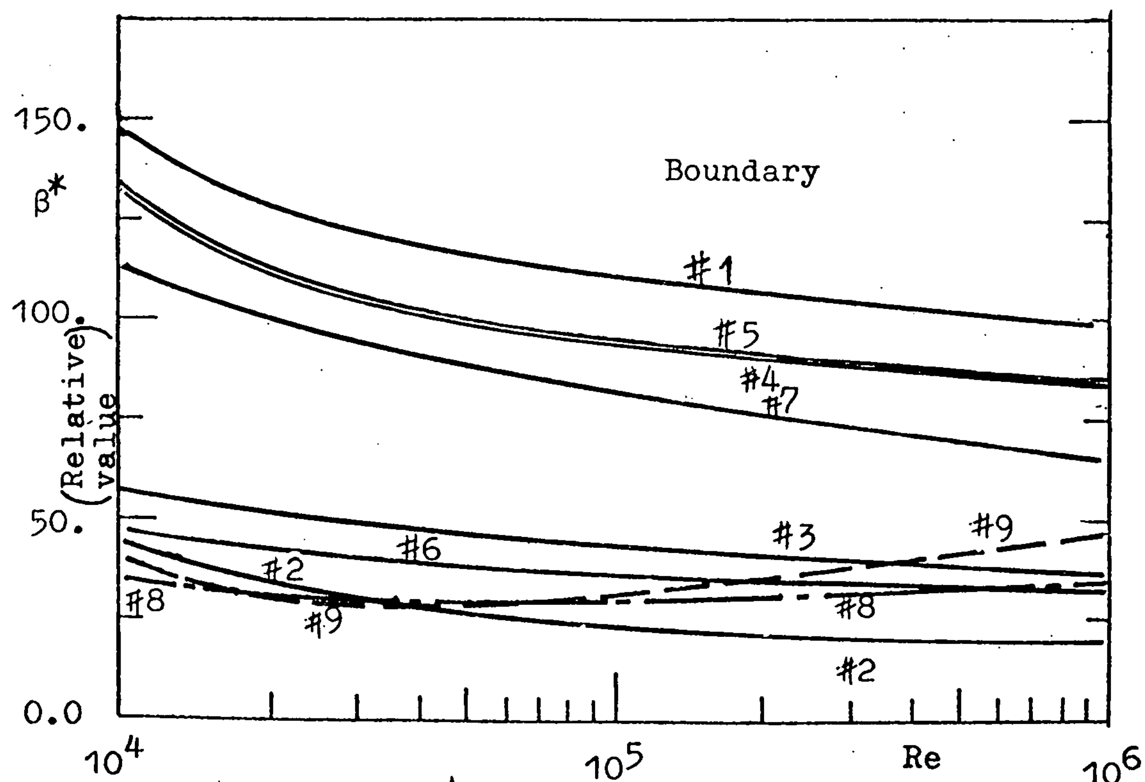


Fig. 15-2 $\beta^*$ for thirty seven pin bundle, Na coolant at 700°C, rod radius = .25 cm, P/D = 1.25.

## Appendix A

(Taken from Ref. 6)

### VELASCO Description

Essential input information for the solution of the heat transfer problem is the turbulent velocity distribution. The latter is obtained using the computation procedure outlined in detail by the authors. The main features of this procedure can be summarized as follows:

- The bundle flow section is divided into zones pertaining to opposite rod/wall surfaces and separated by lines across which the momentum flux is zero. The continuity of axial coolant velocity at the separation line is a criterion for establishing the position of this line.
- A momentum balance for a differential volume element rd $\phi$ dr dz in zone i leads, for conditions of fully developed flow to:

$$\frac{\partial(\tau_r r)}{\partial r} + \frac{\partial \tau_\phi}{\partial \phi} = \frac{4}{d_{e.i}} \tau_{w.av.i} r \qquad (1)$$

  where $d_{e.i}$ is the hydraulic diameter of zone i and $\tau_{w.av.i}$ is the circumferentially averaged shear stress at the wall associated with zone i.
- The momentum fluxes $\tau_r$ and $\tau_\phi$ incorporate transport contributions due to viscous effects, turbulent velocity

fluctuations, and secondary flow. This is expressed by:

$$\tau_r = -\rho\nu \frac{\partial u}{\partial r} + \rho \overline{u'v'_r} + \rho\, uv_r \qquad (2)$$

$$\tau_\phi = -\rho\nu \frac{\partial u}{r\partial \phi} + \rho \overline{u'v'}_\phi + \rho\, uv_\phi \qquad (3)$$

- The turbulent flux terms $\overline{u'v'_r}$ and $\overline{u'v'_\phi}$ representing one-point correlations between mutually perpendicular velocity fluctuations, are, as usually, related to the time average gradients of the axial coolant velocity u by:

$$u'v'_r = -\varepsilon_{m.r} \frac{\partial u}{\partial r} \quad (4a) \qquad u'v'_\phi = -\varepsilon_{m.\phi} \frac{\partial u}{r\partial \phi} \qquad (4b)$$

where $\varepsilon_{m.r}$ and $\varepsilon_{m.\phi}$ are momentum turbulent diffusivities.

- In the viscous region close to the wall ($0 \leq y^+ \leq 45$) the velocity distributon normal to the wall is given by:

$$u^+ = y^+ - 0.3392 \frac{(y^+)^2}{u_e^+} + 0.039 \frac{(y^+)^3}{(u_e^+)^2} \qquad (5)$$

with $u_e^+ = 14.7$.

Here $u^+$ and $y^+$ are dimensionless velocity and distance parameters, defined by:

$$u^+ = \frac{u}{(\tau_w/\rho)^{1/2}} \quad (6a) \qquad y^+ = \frac{y(\tau_w/\rho)^{1/2}}{\nu} \qquad (6b)$$

- With information availabel on the turbulent momentum transport properties and taking account of Eqn. (5), an expression can be derived for the velocity distribution normally to the wall in terms of $u^+$ and $y^+$.

- Taking account of the fact that momentum fluxes normally to lines separating adjacent flow zones are zero, Eqn. (1) can be radially integrated to give:

$$\frac{\tau_w}{\tau_{w.av.i}} = \frac{y_e}{d_{e.i}} - \frac{d}{d\phi}\left\{\int_o^{y_o/R} \frac{\tau_\phi}{\tau_{w.av.i}}\, d\left(\frac{y}{R}\right)\right\} \qquad (7)$$

where $\tau_w$, $y_e$ and $y_o$ are the wall shear stress, the local hydraulic diameter and the normal distance between wall and zone boundary at a given circumferential position $\phi$. The circumferential momentum transport term $\tau_\phi$ is related to the radial velocity distribution making use of Eqn. (3).

- The wall shear stress $\tau_w/\tau_{w.av.i}$ is expressed in terms of a Fourier series expression. The yet unknown coefficients in this expression are determined by applying Eqn. (7), or a circumferentially integrated version of Eqn. (7) at discrete circumferential positions $\phi$ (point matching). This provides the possibility to determine the velocity field in the various flow zones.

- The above procedure is repeated a number of times in the iterative process of establishing the position of the zone boundaries.

The VELASCO computer programme, of which a listing and description has been given in Ref. [4], has been developed on the above principles. This programme has been applied for the numerical examples presented in this paper.

## Appendix B

### Modifications to VELASCO

Several changes to original "VELASCO" have been made. The modified VELASCO differs from the original in:

1) That a print-out of velocity field is optional since it is expensive to request using the IBM-370 system at MIT-IPC.

2) That instead of print-out, card-output option is added which provides the value of velocity at any specified mesh point for ease in computing the velocity gradient as described in Chapter 3.

3) Card output of subchannel bulk velocity occurs right after the intermediate result punch out.

The whole package of input cards is composed as follows:

Card Y
Card Z
Card A
Card B
NTITLE* Card C
Card 1'
Card 2'
Card 3
Card 4
Card 5
Card 6
NZ* { Card I
Card II*NUZ
Card III*(NUZ+1) }
NUK* Card IV
Card 7

Card Y: (2D15.7)

| Symbol | Meaning |
|---|---|
| RDMS1 | Radial mesh size in viscose wall region |
| RDMS2 | Radial mesh size in turbulent region |

Card Z

| Symbol | | Meaning |
|---|---|---|
| NNVEL | 0 | no card output except the intermediate results |
| | 1 | option for final results in card output |

Card 1'

NWRIZY, NDIFWR, NFIRE 1 have the same significance as given in original "VELASCO".

| Symbol | Meaning |
|---|---|
| NFIRE2 | Selection number, no significance for NFIRE1 = 0; |
| NFIRE1=1 | |
| NFIRE2=1(0) | Signifies the option for output format (no calculation of final results) |
| NFIRE3 | No significance if NFIRE2=0<br>NFIRE2=1; NFIRE3=1(0) signigies the both card output and print output (card output only). |

Card 2'

| Symbol | Meaning |
|---|---|
| TIT | Time in hundredth of seconds which is estimated to be needed for the whole job run. |

See Ref. [4] for cards A, B, C, 3, 4, 5, 6, I, II, III, IV, 7:

The card output will be arranged in the following order:

---

Intermediate results for an eventual continuation [Ref. 4]

---

Subchannel bulk velocity (5D14.6)

---

NUZ* {
- Zone number (I3)
- NCR* {
  - Position number, number and size of meshes at both viscose wall and turbulent region, peripheral position (3I3, 3D15.8)
  - Velocity fields (5D15.8)
  - Distance of zero shear line from the wall and the velocity on this line (45X, 2D15.8)

Remarks on VELASCO Output

i) Of the cases run in this paper, fairly big mesh size in the radial direction has been chosen properly to meet the capacity of the computer. We also eliminate the effort of finding the fine structure of velocity field in the viscous wall region, since it is not important in the integration along the gap because of the negligible thickness of this region.

ii) The velocity fields given by VELASCO are always dimensionless, i.e., every velocity is divided by an averaged velocity of the overall channel of interest.

When these outputs are used for further computations in this paper, we multiply Re x $10^{-5}$ with these velocity fields to give the normalized velocity fields for each bundle case, i.e., u = (U/UB(TOT)) x Re x $10^{-5}$ where U/UB(TOT) is the output form of VELASCO.

iii) The radial distance in VELASCO is also normalized by a reference length R, fuel pin radius. Therefore it should be noted that $W_{ij}^{*M}$'s are calculated originally based on dimensionless length and velocity fields. Also the peripheral distance is divided by each peripheral zone length (in VELASCO either rod or duct circumference). Therefore users should be careful when they perform differentiation, integration or other arithmatic operations.

iv) The subroutine "VELOC" which follows is added to VELASCO to yield the velocity field on punched cards.

```
      SUBROUTINE  VELOC(LK,RDMS1,RDMS2,      IZ,IC,NFIRE3,YPMMX)
      IMPLICIT REAL*8(A-H,O-Z)
      COMMON  /CYCL/NZ,NCR
      COMMON  /NAGARE/YPM,DHTOT,WUT,RET,RF,UDELTA,UMAX,YMZC
      COMMON  /OUTPT/IZB,XT
      COMMON  /ROUGH/ CA,CE,DUR,TE
      DIMENSION   YY(50),UU(50),UUV(8,50),YYT(8),UDELT(8)
      DIMENSION   IZB(8),XT(8),KRAD(8),UUMAX(8) ,YMZ(8)
      DIMENSION   YV(8,50)
      LA=LK
      UDELT(LA)=UDELTA
      YMZ(LA)=YMZC
      IF(YPM.GT.21.)  UUMAX(LA)=UMAX
      IF(YPM.LE.21.)  UUMAX(LA)=0.
      YPD=YPM
      IF(YPM-21.)  1000,1000,1010
 1000 YYT(LA)=2.*YPD*DHTOT/(WUT*RET)
C     IT IS RECOMMENDED TO GIVE FIRST  COARSE MESH SIZE RDMS1 TO AVOID
C     EXCEEDING THE ARRAY SIZE BEING DEFINED BY A PROGRMMER,AND GIVE
C     FINER MESH SIZE FOR WALL REGION IF NECESSARY.
      MMRAD=YYT(LA)/RDMS1
      IF(MMRAD)  1003,1003,1005
 1003 UU(1)=WUT*YPD/RF*(1.-.02313*YPD*(1.-.007804*YPD))
      MRAD=1
      GO TO 1060
 1005 CONTINUE
      MRAD=MMRAD
      GO TO 1020
C     YY(I)=(SMALL R-LARGE R)/LARGE R
C     ARRAY Y  IN MAIN PROGRAM IS  INTERPRETED AS  YY/YM   OR
C     (SMALL R-LARGE R)/(SMALL RM-LARGE R)
C     YMZC=YM IN MAIN PROGRAM I.E. =(SMALL RM-LARGE R)/LARGE R
 1010 YPD=21.
      IF(LA.GT.8) WRITE(6,8050)  LA
 8050 FORMAT(1H0,' +++++++++CHECK OF SUBSCRIPTS  OF YYT --- LA =',I4,'+
     1+++++++++'//)
      YYT(LA)=2.*YPD*DHTOT/(WUT*RET)
      MMRAD=YPMMX/RDMS1
      IF(MMRAD)  1014,1014,1015
 1014 MRAD=YMZC/RDMS2
      GO TO 1016
 1015 MRAD=(YMZC-YPMMX)/RDMS2
 1016 CONTINUE
      MRAD=MMRAD+MRAD
      FNL=1.
      IF(MMRAD.EQ.0)  GO TO 1055
 1020 DO 1050 I=1,MMRAD
      YY(I)=DFLOAT(I)*RDMS1
      IF(YPM-21.)  1030,1030,1040
 1040 FNL=(DLOG(YPD*TE/2.  *(2.  -YPD/YPM)/(1.  +(TE-1.  )*(1.  -YPD/YPM
     1)**2))/CA+CE+DUR)/12.471
      IF(FNL.LT.0.   ) FNL=1.D-6
 1030 YPZ=YY(I)/YMZC
      UU(I)=WUT*YPZ*YPM/RF*(1.-.2313D-1*YPZ*YPM*(1.-.7804D-2*YPZ*YPM))*F
     1NL
```

```
 1050 CONTINUE
 1055 IF(YPM-21.)  1060,1060,1070
 1070 II=MMRAD+1
      DO 1080 I=II,MRAD
      III1=I-II+1
      YY(I)=DFLOAT(MMRAD)*RDMS1+DFLOAT(III1)*RDMS2
      YPZ =YY(I)/YMZC
      UU(I)=UMAX+WUT*DLOG(YPZ *(2.-YPZ )/(1.+(TE-1.)*(1.-YPZ )*(1.-YPZ )
     1))/(CA*RF)
 1080 CONTINUE
 1060 CONTINUE
      DO 1090 I=1,MRAD
      YV(LA,I)=YY(I)
 1090 UUV(LA,I)=UU(I)
C
C     WRITING   BOTH CARDS AND PRINT
      IF (IC.EQ.1)  WRITE(7,8065) IZ
      WRITE(7,8060) IC,MMRAD,MRAD,RDMS1,RDMS2,XT(LA)
      WRITE(7,8070)  (UU(I),I=1,MRAD)
      WRITE(7,8080) YMZC,UMAX
 8060 FORMAT(3I3,3D15.8)
 8065 FORMAT(I3)
 8070 FORMAT(5D15.8)
 8080 FORMAT(45X,2D15.8)
      KRAD(LA)=MRAD
      IF(LA-2)  1092,1093,1093
 1093 MRMX=MAX0(KRAD(LA),MRMX)
      GO TO 1095
 1092 MRMX=KRAD(LA)
 1095 CONTINUE
      IF(IZ.EQ.NZ.AND.IC.EQ.NCR)  GO TO 1100
      IF (LA.LT.8) GO TO 2000
 1100 IF (LA.LT.5) LEND=LA
      IF (LA.GT.4) LEND=4
      NLA=0
      IF(NFIRE3.EQ.0)  GO TO 2000
      WRITE(6,8000)
 1110 WRITE(6,8010)  IZB(1+NLA),XT(1+NLA)
      IF (LEND.EQ.(1+NLA)) GO TO 1120
      WRITE(6,8011)  IZB(2+NLA),XT(2+NLA)
      IF (LEND.EQ.(2+NLA)) GO TO 1120
      WRITE(6,8012)  IZB(3+NLA),XT(3+NLA)
      IF (LEND.EQ.(3+NLA)) GO TO 1120
      WRITE(6,8013)  IZB(4+NLA),XT(4+NLA)
 1120 WRITE(6,8020)
      IF (LEND.EQ.(1+NLA)) GO TO 1130
      WRITE(6,8021)
      IF (LEND.EQ.(2+NLA)) GO TO 1130
      WRITE(6,8022)
      IF (LEND.EQ.(3+NLA)) GO TO 1130
      WRITE(6,8023)
 1130 WRITE(6,8030)
      DO 1140 I=1,MRMX
      WRITE(6,8030)
      IF(KRAD(1+NLA).GE.I)  WRITE(6,8081) YV(1+NLA,I),UUV(1+NLA,I)
```

```
      IF(LEND.EQ.(1+NLA))  GO TO 1140
      IF(KRAD(2+NLA).GE.I)  WRITE(6,8082) YV(2+NLA,I),UUV(2+NLA,I)
      IF(LEND.EQ.(2+NLA))  GO TO 1140
      IF(KRAD(3+NLA).GE.I)  WRITE(6,8083) YV(3+NLA,I),UUV(3+NLA,I)
      IF(LEND.EQ.(3+NLA))  GO TO 1140
      IF(KRAD(4+NLA).GE.I)  WRITE(6,8084) YV(4+NLA,I),UUV(4+NLA,I)
 1140 CONTINUE
      YMAX=1.
      WRITE(6,8031)
      WRITE(6,8030)
      WRITE(6,8081)  YYT(1+NLA),UDELT(1+NLA)
      IF(LEND.EQ.(1+NLA))  GO TO 1150
      WRITE(6,8082)  YYT(2+NLA),UDELT(2+NLA)
      IF(LEND.EQ.(2+NLA))  GO TO 1150
      WRITE(6,8083)  YYT(3+NLA),UDELT(3+NLA)
      IF(LEND.EQ.(3+NLA))  GO TO 1150
      WRITE(6,8084)  YYT(4+NLA),UDELT(4+NLA)
 1150 CONTINUE
      IF(YPM.GE.21.)  WRITE(6,8030)
      IF(YPM.GE.21.)  WRITE(6,8081)  YMZ(1+NLA),UUMAX(1+NLA)
      IF(LEND.EQ.(1+NLA))  GO TO 1160
      IF(YPM.GE.21.)  WRITE(6,8082)  YMZ(2+NLA),UUMAX(2+NLA)
      IF(LEND.EQ.(2+NLA))  GO TO 1160
      IF(YPM.GE.21.)  WRITE(6,8083)  YMZ(3+NLA),UUMAX(3+NLA)
      IF(LEND.EQ.(3+NLA))  GO TO 1160
      IF(YPM.GE.21.)  WRITE(6,8084)  YMZ(4+NLA),UUMAX(4+NLA)
 1160 CONTINUE
      IF(LA.LE.LEND) LA=0
      IF(LA.LE.LEND) GO TO 2000
      NLA=4
      LEND=LA
      GO TO 1110
 8000 FORMAT(////5X,'VELOCITY FIELD VS. CYLINDRICAL CORD.'/)
 8010 FORMAT(///  9X,'ZONE',I2,', X=',F6.4)
 8011 FORMAT('+',39X,'ZONE',I2,', X=',F6.4)
 8012 FORMAT('+',69X,'ZONE',I2,', X=',F6.4)
 8013 FORMAT('+',99X,'ZONE',I2,', X=',F6.4)
 8020 FORMAT('0', 9X,'Y',14X,'U/UB')
 8021 FORMAT('+',39X,'Y',14X,'U/UB')
 8022 FORMAT('+',69X,'Y',14X,'U/UB')
 8023 FORMAT('+',99X,'Y',14X,'U/UB')
 8030 FORMAT(' ')
 8031 FORMAT(' ','***  YYT VS UDELTA  ***   AND'/' ***   YM VS UMAX    *
     1**')
 8081 FORMAT('+',2F15.5)
 8082 FORMAT('+',30X,2F15.5)
 8083 FORMAT('+',60X,2F15.5)
 8084 FORMAT('+',90X,2F15.5)
 2000 RETURN
      END
```

## Appendix C

### Input Data Listing for 19, 37, 61 and 91 Pin Bundles

The author would like to give several brief comments on preparing the input data sets, especially for 61 and 91 pin bundles, since these big size bundles contain more closed flow zones which are surrounded by zero shear lines.

1) The numerical values of the geometrical parameters, i.e., ACH, ACH1, ACH2, ACH3, BCH1, BCH2, BCH3 and BCH4 should be exact (i.e., 6 to 8 digits beyond decimal), otherwise a tiny input error causes seriously erroneous results and sometimes the computation stops due to numerical inconsistency.

2) The choice of the origin for the peripheral coordinate (X=0) should be made to avoid situations such that IXG1, IXG2 or IXG3 is 1 or equal to the last consecutive number of the subzone boundary position at the boundary position of IXGACT = 6.

3) Generally the numbering of zone and subzone boundary positions are arbitrary except for a few limitations as given above.

4) For 61 and 91 pins, further studies are needed since convergent solutions have not been attained after a considerable number of iterations with the input as prepared below.

Following are the lists of input data to VELASCO.

Case 4

```
0.02            0.02
   2
   0     0     1     1
   2
VELOCITY DISTRIBUTION IN A HEXAGONAL NINETEEN  - ROD BUNDLES
  P/D = 1,25      PW/D =1,15
   0     1     1     1     0
100.
  20
5       -03
1       +06
   5    10     5
  21     4     0     1     10.97094   0.0        0.0
   3     1     2     1     0      00.3        0.0        1.0
   3     2     3     3     1      00.3        0.0        1.0
   3     3     3     2     0      10.3        0.0        1.0
   3     4     3     1     1      00.45789    -3.57143   1.0
3  2  1                             0.0        0.0        0.3
6  1  2  3  2  2  4  1 -1  1        0.3        0.5        0.3        0.0
3  3  3                             0.772654   0.166667   0.3
4  1  3  4  2 -1  1                 0.954691   0.3        0.0        1.0
3  3  1                             1.0        0.0        0.45789
  25     5     0     1     11.0         1        -061.0
   2     1     1     1     0      00.3        1.0        0.0
   3     5     3     4     1      10.5        1.0        1.0
   3     6     3     5     0      00.5        1.0        1.0
   3     7     4     2     1      10.5        1.0        1.0
   3     8     4     3     0      00.5        1.0        1.0
1
1
3  3  5                             0.5        0.666667   0.5
6  2  3  4  4  6  2  1 -1 -1        0.5        0.5        0.5
3  4  3                             0.833333   0.333333   0.5
4  2  4  6  4 -1 -1                 1.0        0.5        1.0        1.0
  25     6     0     1     11.0         1        -061.0
   2     4     1     4     0      10.45789    1.0        -3.57143
   2     3     1     3     1      00.3        1.0        0.0
   2     2     1     2     0      10.3        1.0        0.0
   2     5     2     2     1      10.5        1.0        1.0
   2     6     2     3     0      00.5        1.0        1.0
   3     9     4     1     1      00.5        1.0        1.0
1
1
1
1
1
1
3  4  1                             1.0        0.0        0.5
  25     6     0     1     11.0         1        -061.0
   2     9     3     6     0      10.5        1.0        1.0
   2     7     2     4     1      10.5        1.0        1.0
   2     8     2     5     0      00.5        1.0        1.0
   1                       1      00.5        1.0        1.0
   1                       0       0.5        1.0        1.0
   3    10     5     1     1      00.5        1.0        1.0
1
1
1
1
```

```
2                                             0.666667  0.25
1   5  4  2  6 -1  1                          1.0       0.5       1.0       1.0
3   5  1                                      1.0       0.0       0.5
    5     1     0     1    16.0         1         -061.0
    2    10     4     6     0    10.5        1.0          1.0
1
1                                                                 5     3               9
    2     1     3                      3     1                    3     3     5        17
    3     1     2     3                1     1     3              5     7     3         9
    3     2     3     4                3     5     1              6     5               9
    2     2     4                      5     3                    7     2               9
    2     4     5                      5     1
    0
```

61 pins
Re=$10^5$

```
0.02            0.02
    2
    0     0     3     1
    2
VELOCITY DISTRIBUTION IN A HEXAGONAL SIXTY ONE - ROD BUNDLES
   P/D = 1.25       W/D =1.15
    0     1     1     1     0
480.
   20
 1      -02
 1      +06
   10    30    13
   33     6     0     1     1   .547735    .0          .0
    3     1     2     1     0     0    .3         .0         1.0
    3     2     3    10     1     1    .3         .0         1.0
    3     3     3     1     0     0    .3         .0         1.0
    3     4     4     3     1     0    0.3        0.         1.
    3     5     4     2     0     1    .3         0.         1.
    3     6     4     1     1     0    .45789  -3.57143   1.
 3  2  1  0  0  0  0  0  0  0   00.          0.0        0.3        0.0
 6  1  2  3  2  2 10 -1  1  1   00.3         0.5        0.3        0.0
 3  3  1  0  0  0  0  0  0  0   00.435874    0.0        0.3        0.0
 6  1  3  4  4  2  4 -1  1 -1   00.3         0.5        0.3        0.0
 3  4  3  0  0  0  0  0  0  0   00.871748    0.166667   0.3        0.0
 4  1  4  6  2 -1  1  0  0  0   00.974440    0.3        0.0        1.0
 3  4  1  0  0  0  0  0  0  0   01.0         0.0        0.45789    0.0
   25     5     0     1     11.0         1       -061.0
    2     1     1     1     0     00.3       1.0        0.0
    3    14     3     9     1     00.5       1.0        1.0
    3    13     3     8     0     10.5       1.0        1.0
    3    15     5    11     1     00.5       1.0        1.0
    3    16     5    10     0     10.5       1.0        1.0
 1
 1
 3  3  9                         0.5        0.75       0.5
 6  2  5  3  4 12  8  1  1  1    0.5        0.5        0.5
 3  5 11                         0.833333   0.833333   0.5
 4  2  5  6 10 -1  1             1.0        0.5        1.0        1.0
   49    10     1     1     10.5         1       -061.
    2     3     1     3     0     00.3       1.0        0.0
    3     7     4     4     1     10.5       1.0        1.0
    3     8     4     5     0     00.5       1.0        1.0
    3     9     6     2     1     10.5       1.0        1.0
    3    10     6     3     0     00.5       1.0        1.0
    3    11     5     1     1     00.5       1.0        1.0
    3    12     5    12     0     10.5       1.0        1.0
    2    13     2     3     1     00.5       1.0        1.0
    2    14     2     2     0     10.5       1.0        1.0
    2     2     1     2     1     10.3       1.0        1.0
 1
 1
 3  4  5                         0.25       0.666667   0.5
 6  3  4  6  4  6  2 -1  1  1    0.5        0.5        0.5
 3  6  3                         0.416667   0.333333   0.5
 6  3  5  6  6  2  4  1  1 -1    0.5        0.5        0.5
 3  5  1                         0.583333   0.0        0.5
 1
 1
 1
```

```
3  1  3                                    1.0       0.435874  0.3         0.0
  25    6    0     1    11.0         1       -061.0
   2    6    1     6    0     10.45789    1.0         -3.57143
   2    5    1     5    1     00.3        1.0         0.0
   2    4    1     4    0     10.3        1.0         0.
   2    7    3     2    1     10.5        1.0         1.0
   2    8    3     3    0     00.5        1.0         1.0
   3   17    6     1    1     00.5        1.0         1.0
1
1
1
1
1
1
3  6  1                                    1.0       0.0       0.5
  49   12    1     1    10.5         1       -061.0
   2   11    3     6    0     10.5        1.0         1.0
   3   18    6     4    1     10.5        1.0         1.0
   3   19    6     5    0     00.5        1.0         1.0
   3   20    8     2    1     10.5        1.0         1.0
   3   21    8     3    0     00.5        1.0         1.0
   3   22    7     2    1     00.5        1.0         1.0
   3   23    7     1    0     10.5        1.0         1.0
   1                    1      0.5        1.0         1.0
   1                    0      0.5        1.0         1.0
   2   16    2     5    1     00.5        1.0         1.0
   2   15    2     4    0     10.5        1.0         1.0
   2   12    3     7    1     00.5        1.0         1.0
1
1
3  6  5                                    0.166667  0.666667  0.5
6  5  6  8  4  6  2 -1  1  1               0.5       0.5       0.5
3  8  3                                    0.333333  0.333333  0.5
6  5  7  8  6  3  4  1  1 -1               0.5       0.5       0.5
3  7  2                                    0.5       0.166667  0.5
4  7  5  1  8  1 -1                        0.0       0.5       1.0         1.0
2                                          0.666667  0.25
1
1
1
3  3  7                                    1.0       0.583333  0.5
  25    6    0     1    11.0         1       -061.0
   2   17    4     6    0     10.5        1.0         1.0
   2    9    3     4    1     10.5        1.0         1.0
   2   10    3     5    0     00.5        1.0         1.0
   2   18    5     2    1     10.5        1.0         1.0
   2   19    5     3    0     00.5        1.0         1.0
   3   24    8     1    1     00.5        1.0         1.0
1
1
1
1
1
1
3  8  1                                    1.0       0.0       0.5
  25    6    0     1    11.0         1       -061.0
   2   23    5     7    1     00.5        1.0         1.0
   2   22    5     6    0     10.5        1.0         1.0
   3   25    8     4    1     10.5        1.0         1.0
```

```
   3   26    8    5    0   00.5       1.0       1.0
   3   27    9    2    1   10.5       1.0       1.0
   3   28    9    3    0   00.5       1.0       1.0
1
1
1
3  8  5                       0.5       0.666667  0.5
6  7  8  9  5  6  2 -1  1  1  0.5       0.5       0.5
3  9  3                       0.833333  0.333333  0.5
4  7  9  7  4 -1 -1           1.0       0.5       1.0       1.0
  25    6    0    1   11.0        1      -061.0
   2   24    6    6    0   10.5       1.0       1.0
   2   20    5    4    1   10.5       1.0       1.0
   2   21    5    5    0   00.5       1.0       1.0
   2   25    7    3    1   10.5       1.0       1.0
   2   26    7    4    0   0 .5       1.0       1.0
   3   29    9    1    1   00.5       1.0       1.0
1
1
1
1
1
1
3  9  1                       1.0       0.0       0.5
  25    6    0    1   11.0        1      -061.0
   2   29    8    6    0   10.5       1.0       1.0
   2   27    7    5    1   10.5       1.0       1.0
   2   28    7    6    0   0 .5       1.0       1.0
   1                   1    0.5       1.0       1.0
   1                   0    0.5       1.0       1.0
   3   30   10    1    1   00.5       1.0       1.0
1
1
1
1
2                             0.666667  0.25
4 10  9  2  6 -1  1           1.0       0.5       1.0       1.0
3 10  1                       1.0       0.0       0.5
   5    1    0    1   16.0        1      -061.0
   2   30    9    6    0   10.5       1.0       1.0
1
1
   2    1    4             5    1             7    3            9
   3    1    3    4        3    1    3        5    3    5      17
   3    1    2    3        1    1    9        3    3   11      17
   3    3    4    6        3    5    1        5    7    3      17
   3    2    3    5        3    7   11        5    9   13       9
   3    3    5    6        5    1    3        7    3    5       9
   2    2    5             5    9             6   11            9
   3    5    6    8        3    5    1        5    7    3       9
   2    5    7             7    1             9    2            9
   3    5    7    8        5    2    3        7    4    5       9
   3    7    8    9        4    5    1        6    7    3       9
   2    7    9             6    3             7    5            9
   2    9   10             5    1             7    2            9
  20
0.02           0.02
   2
```

```
0.02            0.02                                         91 pins,Re =10^5
   2
   0     0     4     1
   2
VELOCITY DISTRIBUTION IN A HEXAGONAL NINTY ONE - ROD BUNDLES
   P/D = 1.25      PW/D =1.15
   0     1     1     1     0
800.
   10
 1     -02
 1     +06
   13    44    19
   37     7     0     1     10.449724  0.0          0.0
    3     1     2    10     1     10.3         0.0          1.0
    3     2     2     1     0     00.3         0.0          1.0
    3     3     3    10     1     10.3         0.0          1.0
    3     4     3     1     0     00.3         0.0          1.0
    3     5     4     3     1     00.3         0.0          1.0
    3     6     4     2     0     10.3         0.0          1.0
    3     7     4     1     1     00.45789     -3.57143     1.0
 4  1  2  1 10  1  1                 0.0         0.3          0.0          1.0
 3  2  1                             0.178939    0.0          0.3
 6  1  2  3  3  2 10 -1  1 -1        0.3         0.5          0.3
 3  3  1                             0.536818    0.0          0.3
 6  1  3  4  5  2  4 -1  1 -1        0.3         0.5          0.3
 3  4  3                             0.894697    0.166667     0.3
 4  1  4  7  2 -1  1                 0.979135    0.3          0.0          1.0
 3  4  1                             1.0         0.0          0.45789
   49    10     1     1     10.5          1       -061.
    2     2     1     2     0     00.3         1.0          0.0
    3    15     3     9     1     00.5         1.0          1.0
    3    14     3     8     0     10.5         1.0          1.0
    3    16     6    11     1     00.5         1.0          1.0
    3    17     6    10     0     10.5         1.0          1.0
    3    18     5     2     1     00.3         1.0          1.0
    3    19     5     1     0     10.5         1.0          1.0
    1                       1      0.5         1.0          1.0
    1                       0      0.5         1.0          1.0
    2     1     1     1     1     10.3         1.0          0.0
1
1
3  3  9                              0.25        0.75         0.5
6  2  6  3  4 12  8  1  1  1         0.5         0.5          0.5
3  6 11                              0.416667    0.833333     0.5
6  2  5  6  6  3 10  1  1  1         0.5         0.5          0.5
3  5  2                              0.583333    0.166667     0.5
4  5  2  1  8  1 -1                  0.0         0.5          1.0          1.0
2                                    0.75        0.25
1
3  1  2                              1.0         0.178939     0.3
   49    10     1     1     10.5          1       -061.
    2     4     1     4     0     00.3         1.0          0.0
    3     8     4     4     1     10.5         1.0          1.0
    3     9     4     5     0     00.5         1.0          1.0
    3    10     7     2     1     10.5         1.0          1.0
    3    11     7     3     0     00.5         1.0          1.0
    3    12     6     1     1     00.5         1.0          1.0
    3    13     6    12     0     10.5         1.0          1.0
    2    14     2     3     1     00.5         1.0          1.0
```

```
    2   15    2    2    0   10.5        1.0        1.0
    2    3    1    3    1   10.3        1.0        0.0
1
i
3   4   5                             0.25        0.666667   0.5
6   3   4   7   4   6   2  -1   1   i   0.5         0.5        0.5
3   7   3                             0.416667    0.333333   0.5
6   3   6   7   6   2   4   1   1  -1   0.5         0.5        0.5
3   6   1                             0.583333    0.0        0.5
1
1
1
3   1   4                             1.0         0.536818   0.3
   25    6    0    1   11.0          1       -061.0
    2    7    1    7    0   10.45789    1.0        -3.57143
    2    6    1    6    1   00.3        1.0        0.0
    2    5    1    5    0   10.3        1.0        0.0
    2    8    3    2    1   10.5        1.0        1.0
    2    9    3    3    0   00.5        1.0        1.0
    3   20    7    1    1   00.5        1.0        1.0
1
1
1
1
1
1
3   7   1                             1.0         0.0        0.5
   25    6    0    1   11.0          1       -061.0
    2   19    2    7    1   00.5        1.0        1.0
    2   18    2    6    0   10.5        1.0        1.0
    3   28    6    9    1   00.5        1.0        1.0
    3   27    6    8    0   10.5        1.0        1.0
    3   30    8   11    1   00.5        1.0        1.0
    3   31    8   10    0   10.5        1.0        1.0
1
1
1
3   6   9                             0.5         0.666667   0.5
6   5   8   6   5  12   8   1   1   1   0.5         0.5        0.5
3   8  11                             0.833333    0.833333   0.5
4   5   8   7  10  -1   1               1.0         0.5        1.0        1.0
   49   12    1    1   10.5          1       -061.0
    2   12    3    6    0   10.5        1.0        1.0
    3   21    7    4    1   10.5        1.0        1.0
    3   22    7    5    0   00.5        1.0        1.0
    3   23    9    2    1   10.5        1.0        1.0
    3   24    9    3    0   00.5        1.0        1.0
    3   25    8    1    1   00.5        1.0        1.0
    3   26    8   12    0   10.5        1.0        1.0
    2   27    5    4    1   00.5        1.0        1.0
    2   28    5    3    0   10.5        1.0        1.0
    2   17    2    5    1   00.5        1.0        1.0
    2   16    2    4    0   10.5        1.0        1.0
    2   13    3    7    1   00.5        1.0        1.0
1
1
3   7   5                             0.166667    0.666667   0.5
6   6   7   9   4   6   2  -1   1   1   0.5         0.5        0.5
3   9   3                             0.333333    0.333333   0.5
```

```
6  6  8  9  6  2  4  1  1 -1   0.5        0.5        0.5
3  8  1                        0.5        0.0        0.5
1
1
1
1
1
3  3  7                        1.0        0.583333   0.5
  25    6    0    1    11.0         1     -061.0
   2   20    4    6    0    10.5       1.0        1.0
   2   10    3    4    1    10.5       1.0        1.0
   2   11    3    5    0    00.5       1.0        1.0
   2   21    6    2    1    10.5       1.0        1.0
   2   22    6    3    0    00.5       1.0        1.0
   3   29    9    1    1    00.5       1.0        1.0
1
1
1
1
1
1
3  9  1                        1.0        0.0        0.5
  49   12    1    1    10.5         1     -061.0
   2   25    6    6    0    10.5       1.0        1.0
   3   32    9    4    1    10.5       1.0        1.0
   3   33    9    5    0    00.5       1.0        1.0
   3   34   11    2    1    10.5       1.0        1.0
   3   35   11    3    0    00.5       1.0        1.0
   3   36   10    2    1    00.5       1.0        1.0
   3   37   10    1    0    10.5       1.0        1.0
   1                   1     0.5       1.0        1.0
   1                   0     0.5       1.0        1.0
   2   31    5    6    1    00.5       1.0        1.0
   2   30    5    5    0    10.5       1.0        1.0
   2   26    6    7    1    00.5       1.0        1.0
1
1
3  9  5                        0.166667    .666667   0.5
6  8  9 11  4  6  2 -1  1  1   0.5        0.5        0.5
3 11  3                        0.333333   0.333333   0.5
6  8 10 11  6  3  4  1  1 -1   0.5        0.5        0.5
3 10  2                        0.5        0.166667   0.5
4 10  8  1  8  1 -1            0.0        0.5        1.0        1.0
2                              0.666667   0.25
1
1
1
3  6  7                        1.0        0.5        0.5
  25    6    0    1    11.0         1     -061.0
   2   29    7    6    0    10.5       1.0        1.0
   2   23    6    4    1    10.5       1.0        1.0
   2   24    6    5    0    00.5       1.0        1.0
   2   32    8    2    1    10.5       1.0        1.0
   2   33    8    3    0    00.5       1.0        1.0
   3   38   11    1    1    00.5       1.0        1.0
1
1
1
1
```

```
1
1
3 11   1                                       1.0         0.0         0.5
  25     6     0     1     11.0          1       -061.0
    2    37     8     7     1     00.5         1.0          1.0
    2    36     8     6     0     10.5         1.0          1.0
    3    39    11     4     1     10.5         1.0          1.0
    3    40    11     5     0     00.5         1.0          1.0
    3    41    12     2     1     10.5         1.0          1.0
    3    42    12     3     0     00.5         1.0          1.0
1
1
1
3 11   5                                       0.5         0.666667    0.5
6 10 11 12   5   6   2 -1   1   1              0.5         0.5         0.5
3 12   3                                       0.833333    0.333333    0.5
4 10 12   7   4 -1 -1                          1.0         0.5         1.0         1.0
  25     6     0     1     11.0          1       -061.0
    2    38     9     6     0     10.5         1.0          1.0
    2    34     8     4     1     10.5         1.0          1.0
    2    35     8     5     0     00.5         1.0          1.0
    2    39    10     3     1     10.5         1.0          1.0
    2    40    10     4     0     00.5         1.0          1.0
    3    43    12     1     1     00.5         1.0          1.0
1
1
1
1
1
1
3 12   1                                       1.0         0.0         0.5
  25     6     0     1     11.0          1       -061.0
    2    43    11     6     0     10.5         1.0          1.0
    2    41    10     5     1     10.5         1.0          1.0
    2    42    10     6     0     00.5         1.0          1.0
    1                       1      0.5         1.0          1.0
    1                       0      0.5         1.0          1.0
    3    44    13     1     1     00.5         1.0          1.0
1
1
1
1
2                                              0.666667    0.25
4 13 12   2   6 -1   1                         1.0         0.5         1.0         1.0
3 13   1                                       1.0         0.0         0.5
    5     1     0     1     16.0          1       -061.0
    2    44    12     6     0     10.5         1.0          1.0
1
1
    2     1     4             6     1            8     3            9
    3     1     3     4       4     1     3      6     3     5     17
    3     1     2     3       2     1     9      4     3    11     17
    2     1     2             1     9            2    11           17
    3     3     4     7       3     5     1      5     7     3      9
    3     2     3     6       3     7    11      5     9    13      9
    2     2     5             7     1            9     2            9
    3     3     6     7       5     1     3      7     3     5      9
    3     2     5     6       5     2     9      7     4    11      9
    3     6     7     9       3     5     1      5     7     3      9
```

| | | | | | | | | | | |
|---|---|---|---|---|---|---|---|---|---|---|
| 3 | 5 | 6 | 8 | 4 | 7 | 11 | 6 | 9 | 13 | 9 |
| 3 | 6 | 8 | 9 | 5 | 1 | 3 | 7 | 3 | 5 | 9 |
| 2 | 5 | 8 | | 6 | 9 | | 7 | 11 | | 9 |
| 3 | 8 | 9 | 11 | 3 | 5 | 1 | 5 | 7 | 3 | 9 |
| 2 | 8 | 10 | | 7 | 1 | | 9 | 2 | | 9 |
| 3 | 8 | 10 | 11 | 5 | 2 | 3 | 7 | 4 | 5 | 9 |
| 3 | 10 | 11 | 12 | 4 | 5 | 1 | 6 | 7 | 3 | 9 |
| 2 | 10 | 12 | | 6 | 3 | | 7 | 5 | | 9 |
| 2 | 12 | 13 | | 5 | 1 | | 7 | 2 | | 9 |

52

Appendix D

Listing of the Program for the Mixing Distance $1/Z_{ij}$

```
      DIMENSION  NG(2,20),NSB(2,20),MMRDL(40),MMRDR(40),
     1           MRDL(40),MRDR(40),DX(40),UL(40,50),UR(40,50),
     2           UB(20),DVDX(40,50),MM2(40),MM1(40),YY(50),XI(50),
     3           SUM1(50),SUM2(50),TAUTL(40),TAU(20),YD1(20),YD2(20),
     4           DENM(20),TAUAV(20),TAULIN(20),DUB(20),ZM(20),
     5           MMRDC(40),MRDC(40),UC(40,50),DD(40),TDVDX(40,50),
     6           WIJ(20),EPS(20),AVU(20),BETA(20)
      DOUBLE PRECISION UL,UC,UR,UB
C     NUK --- NUMBER OF SUBCHANNELS
C     NBP ---   **        BOUNDARY POSITIONS
C     NBD ---   **        SUBCHANNEL BOUNDARIES
C     NPERI ---  **       PERIPHERAL POSITIONS
C     NG  --- THE NUMBER OF POSITION OF PAIR BOUNDARIES
C     NSB ---       **        SUBCHANNELS WHICH ARE ADJACENT TO EACH OHTER
C     MMRDL --- NUMBER OF RADIAL MESH POINTS WITHIN THE WALL VISCOUS
C               REGION
C     MMRDC ---                               ***
C     MMRDR ---                               ***
C     MRDL --- NUMBER OF TOTAL MESH POINTS IN RADIAL DIRECTION
C     MRDC ---                              ***
C     MRDR ---                              **
C     R --- RADIUS OF THE ROD
C     RMU --- VISCOSITY OF THE FLUID
C     RNU --- DYNAMIC VISCOSITY
C     PBYD --- =P/D
C     HV --- MESH SIZE IN VISCOSE WALL REGION IN RADIAL DIRECTION
C     HT --- MESH SIZE IN CENTRAL REGION          **
C     DX --- MESH SIZE IN CIRCUMFERENTIAL DIRECTION
C     DD --- DEVIATION OF THE SUBCHANNEL BOUNDARY POSITION
C     RE --- RELATIVE REYNOLDS NUMBER
C     EPS --- DIMENSIONLESS EDDY DIFUSIVITY
C            FROM THE CENTRAL POSITION OF THE THREE
C     UL,UC,AND UR ARE VELOCITIES AT EACH PERIPHERAL POSITION
C            OF THE THREE
C     UB --- SUBCHANNEL BULK VELOCITY
C     ******************************************************************
C     INITIALIZATION
      PI=3.14159
   11 CONTINUE
      DO 900 I=1,40
      MM1(I)=0
      MM2(I)=0
  900 TAUTL(I)=0.
      DO 910 I=1,40
      DO 910 J=1,50
  910 DVDX(I,J)=0.
C     INPUT READING
  500 FORMAT(4I5)
      READ(5,500) NUK,NBP,NBD,NPERI
      DO 1000 I=1,2
 1000 READ(5,500) (NG(I,K),K=1,NBD)
      DO 1005 I=1,2
 1005 READ(5,500) (NSB(I,K),K=1,NBD)
      READ(5,505) (MMRDL(K),MMRDC(K),MMRDR(K) ,K=1,NBP)
      READ(5,505) ( MRDL(K), MRDC(K), MRDR(K) ,K=1,NBP)
```

```
      READ(5,520) R
      READ(5,520) RNU,RMU
      READ(5,520) PBYD
      READ(5,520) HV,HT
      HV=HV*R
      HT=HT*R
      READ(5,520) (DX(I),I=1,NBP)
      READ(5,520) (DD(I),I=1,NBP)
      READ(5,530) NTEST1,NTEST2,NTEST3,NTEST4
      READ(5,520) RE
      READ(5,520) (EPS(I),I=1,NBD)
      DO 1010 I=1,NBP
      DX(I)=DX(I)*PI*R
      DD(I)=DD(I)*PI*R
      LL=MRDL(I)
      READ(5,520) (UL(I,L),L=1,LL)
      DO 1011 L=1,LL
 1011 UL(I,L)=UL(I,L)*RE
      LC=MRDC(I)
      READ(5,520) (UC(I,L),L=1,LC)
      DO 1012 L=1,LC
 1012 UC(I,L)=UC(I,L)*RE
      LR=MRDR(I)
      READ(5,520) (UR(I,L),L=1,LR)
      DO 1013 L=1,LR
 1013 UR(I,L)=UR(I,L)*RE
 1010 CONTINUE
      READ(5,540) (UB(I),I=1,NUK)
      DO 1014 I=1,NUK
 1014 UB(I)=UB(I)*RE
  500 FORMAT(20I3)
  505 FORMAT(3I3)
  520 FORMAT(5D15.8)
  540 FORMAT(5D14.6)
      WRITE(6,605) NTEST1,NTEST2,NTEST3,NTEST4
      WRITE(6,870)
C      ************************************
C
C     CALCULATION OF GRADIENT OF VELUCITY
C
C      ************************************
C1    PERIPHERAL REGION  --- CARTESIAN COORDS.
      DO 1020 I=1,NPERI
      MM1(I)=MIN0(MMRDL(I),MMRDR(I),MMRDC(I))
      MM2(I)=MIN0(MRDL(I),MRDR(I),MRDC(I))
      MM2I=MM2(I)
      DO 1030 J=1,MM2I
      DVDX(I,J)=(UR(I,J)-UL(I,J))/(2.*DX(I))+DD(I)*(UR(I,J)-2.*UC(I,J)+U
     1L(I,J))/(DX(I)*DX(I))
 1030 DVDX(I,J)=ABS(DVDX(I,J))
 1020 CONTINUE
C
C2    INTERIOR REGIN  --- CYLINDRICAL COORDS.
      NINT=NPERI+1
      DO 1040 I=NINT,NBP
      MM1(I)=MIN0(MMRDL(I),MMRDR(I),MMRDC(I))
      MM2(I)=MIN0(MRDL(I),MRDR(I),MRDC(I))
```

```
      MM1I=MM1(I)
      MM2I=MM2(I)
      IF(MM1I.EQ.0) GO TO 1051
      DO 1050 J=1,MM1I
 1050 XI(J)=FLOAT(J)*HV+R
 1051 CONTINUE
      MMII=MM1I+1
      MMKI=MM1I
      IF(MM1I.EQ.0) XI(1)=R
      IF (MM1I.EQ.0) MM1I=1
      DO 1055 J=MMII,MM2I
      XI(J)=XI(MM1I)+FLOAT(J-MMKI)*HT
 1055 CONTINUE
      DO 1058 J=1,MM2I
      DVDX(I,J)=(UR(I,J)-UL(I,J))*R/(2.*DX(I)*XI(J))+DD(I)*(UR(I,J)-2.*U
     1C(I,J)+UL(I,J))*R*R/(DX(I)*DX(I)*XI(J)*XI(J))
 1058 DVDX(I,J)=ABS(DVDX(I,J))
 1040 CONTINUE
C
C        **************************************
C
C     MOMENTUM CROSS FLOW AT THE BOUNDARY POSITION
C
C        **************************************
C     NUMERICAL INTEGRATION
      MX=0
      DO 1060 I=1,NBP
      MM1I=MM1(I)
      MM2I=MM2(I)
      IF(MM1I.EQ.0) GO TO 1075
      DO 1070 J=1,MM1I
 1070 YY(J)=DVDX(I,J)
      SUM1(MM1I)=SEKBN3(YY,HV,MM1I)
 1075 CONTINUE
      MMM=1+MM1I
      DO 1080 J=MMM,MM2I
 1080 YY(J)=DVDX(I,J)
      MDIM=MM2I-MM1I
      SUM2(MDIM)=SEKBN3(YY,HT,MDIM)
      MDIM=MM2I-MM1I
      MX=MAX0(MX,MM2I)
      IF (MM1I.EQ.0) SUM1(1)=0.
      IF(MM1I.EQ.0) MM1I=1
 1090 TAUTL(I)=SUM1(MM1I)+SUM2(MDIM)
 1060 CONTINUE
C
C     COMBINE TWO TAUS WHICH ARE DEFINED ALONG THE SAME BOUNDARY
C     AND COMUPTE THE AVERAGE ALONG THE BOUNDARY.
      DO 1100 K=1,NBD
      NG1=NG(1,K)
      NG2=NG(2,K)
      IF(NG1.EQ.0)  NG1=40
      IF(NG2.EQ.0)  NG2=40
      TAU(K)=TAUTL(NG1)+TAUTL(NG2)
C     YD1 --- DISTANCE FROM ZERO SHEAR TO WALL
      YD1(K)=HV*MM1(NG1)+HT*(MM2(NG1)-MM1(NG1))
C     PERIPHERAL AND INTERIOR REGION
```

```
C      YD2 --- PW/2.-D/2.
       YD2(K)=HV*MM1(NG2)+HT*(MM2(NG2)-MM1(NG2))
       DENM(K)=YD1(K)+YD2(K)
       WRITE(6,880) TAUTL(NG1),TAUTL(NG2),TAU(K)
       WRITE(6,880) YD1(K),YD2(K),DENM(K)
C      AVERAGED TAU
       TAUAV(K)=TAU(K)/DENM(K)
 1100  CONTINUE
C      CALC. OF EXCH. COEF. ALONG THE BOUNDARY (P-D) OR (P/D-1)
C      IN DIMENSIONLESS
C      ****************************************************************
       DO 1200 K=1,NBD
 1200  TAULIN(K)=(PBYD-1.)*TAUAV(K)
C
C      NOTE ;  PBYD MAY CHANGE ACCORDING TO THE DEFINITION OF TAULIN.
C      FOR EXAMPLE, PBYD MAY BE THE LENGTH OF OPEN GAP AND DEPENDS
C      ON THE POSITION OF THE BOUNDARY.
C      CALCULATION OF THE INVERSE MIXING DISTANCE,WIJ,AND BETA.
C      NOTE ;  SELECT SUITABLE SUBCHANNEL BULK VELOCITY
C      TO GET THE DIFFERRNCE OF UB'S CORRESPONDING TO THE BOUNDARY
C      POSITION.
C      ****************************************************************
       DO 1210 K=1,NBD
       NSB1=NSB(1,K)
       NSB2=NSB(2,K)
       DUB(K)=UB(NSB2)-UB(NSB1)
       AVU(K)=(UB(NSB1)+UB(NSB2))*.5
       ZM(K)= -TAUAV(K)/DUB(K)
       WRITE(6,890) K,DUB(K), TAUAV(K),ZM(K)
 1210  CONTINUE
       DO 1220 K=1,NBD
       WIJ(K)= RMU*DENM(K)*(1.+EPS(K))*ZM(K)
       BETA(K)= WIJ(K)/(AVU(K)*DENM(K))
 1220  CONTINUE
C
C      **********
C      * OUTPUT *
C      **********
C
       WRITE(6,600)
       WRITE(6,610) NUK,NBP,NBD,NPERI
       DO 2000 I=1,2
 2000  WRITE(6,610) (NG(I,K),K=1,NBD)
       DO 2005 I=1,2
 2005  WRITE(6,610) (NSB(I,K),K=1,NBD)
       WRITE(6,615) ( MMRDL(K),MMRDC(K) ,MMRDR(K),K=1,NBD)
       WRITE(6,620) R
       WRITE(6,620) RMU,RNU
       WRITE(6,615) (  MRDL(K), MRDC(K)  , MRDR(K),K=1,NBD)
       WRITE(6,620) PBYD
       WRITE(6,620) HV,HT
       WRITE(6,620) (DX(I),I=1,NBP)
       WRITE(6,620) (DD(I),I=1,NBP)
       WRITE(6,620) RE
       WRITE(6,620) (EPS(I),I=1,NBD)
       WRITE(6,625)
       DO 2010 I=1,NBP
```

```
      LL=MRDL(I)
      WRITE(6,630) (UL(I,L),L=1,LL)
      LC=MRDC(I)
      WRITE(6,630) (UC(I,L),L=1,LC)
      LR=MRDR(I)
      WRITE(6,630) (UR(I,L),L=1,LR)
      WRITE(6,625)
 2010 CONTINUE
      WRITE(6,630) (UB(I),I=1,NUK)
      WRITE(6,640)
      WRITE(6,650)
      KKI=1
      KKE=10
      WRITE(6,660)
 3050 CONTINUE
      WRITE(6,670)
      DO 3000 J=1,MX
      WRITE(6,680) J,(DVDX(I,J),I=KKI,KKE)
      DO 3010 K=KKI,KKE
      IF(J-MM1(K)) 3015,3015,3010
 3015 GO TO (1,2,3,4,5,6,7,8,9,10),K
    1 WRITE(6,710)
      GO TO 3010
    2 WRITE(6,720)
      GO TO 3010
    3 WRITE(6,730)
      GO TO 3010
    4 WRITE(6,740)
      GO TO 3010
    5 WRITE(6,750)
      GO TO 3010
    6 WRITE(6,760)
      GO TO 3010
    7 WRITE(6,770)
      GO TO 3010
    8 WRITE(6,780)
      GO TO 3010
    9 WRITE(6,790)
      GO TO 3010
   10 WRITE(6,800)
 3010 CONTINUE
 3000 CONTINUE
      IF(NBP-KKE) 3030,3030,3040
 3040 KKI=KKI+10
      KKE=KKE+10
      GO TO 3050
 3030 WRITE(6,820)
      WRITE(6,640)
      WRITE(6,640)
      WRITE(6,830)
      WRITE(6,690) (TAU(K),K=1,NBD)
      WRITE(6,840)
      WRITE(6,690) (TAUAV(K),K=1,NBD)
      WRITE(6,850)
      WRITE(6,690) (TAULIN(K),K=1,NBD)
      WRITE(6,860)
      WRITE(6,690) (ZM(K),K=1,NBD)
```

```
      WRITE(6,950)
      WRITE(6,690) (WIJ(K),K=1,NBD)
      WRITE(6,960)
      WRITE(6,690) (BETA(K),K=1,NBD)
  600 FORMAT('0',' P1  INPUT DATA '/)
  605 FORMAT(1H1,' *****  C A S E  ***** ', 4I5 /)
  610 FORMAT(1H ,2X,20I3)
  615 FORMAT(1H ,2X,3I3)
  620 FORMAT(1H ,2X,5F16.8)
  625 FORMAT(1H )
  630 FORMAT(1H ,2X,5D14.6)
  640 FORMAT('0')
  650 FORMAT('0',' P2  OUTPUT DATA '/'      VELOCITY GRADIENT NORMAL TO
     1THE SUBCHANNEL BOUNDARIES '/)
  660 FORMAT('0',30X,'S U B C H A N N E L   B O U N D A R Y   P O S I T
     1I O N ')
  670 FORMAT('0',2X,'XI',2X,10(4X,I3,4X))
  680 FORMAT(1H ,2X,I2,2X,10(1X,E10.3))
  690 FORMAT(1H ,6X,10(1X,E10.3))
  710 FORMAT('+',  6X,'*')
  720 FORMAT('+', 17X,'*')
  730 FORMAT('+', 28X,'*')
  740 FORMAT('+', 39X,'*')
  750 FORMAT('+', 50X,'*')
  760 FORMAT('+', 61X,'*')
  770 FORMAT('+', 72X,'*')
  780 FORMAT('+', 83X,'*')
  790 FORMAT('+', 94X,'*')
  800 FORMAT('+',105X,'*')
  820 FORMAT(1H0,'   * INDICATES THE POSITION OF BOUNDARY OF VISCOUS WAL
     1L REGION  ' /)
  830 FORMAT('0',' P3  ----------'/'       MOMENTUM CROSS FLOW'/'     IN
     1 ORDER OF CONSECUTIVE NUMBER OF THE SUBCH. BOUNDARIES' /)
  840 FORMAT('0',' P4  ----------'/'       AV. MOM. CROSS FLOW'/'     IN
     1 ORDER OF CONSECUTIVE NUMBER OF THE SUBCH. BOUNDARIES' /)
  850 FORMAT('0',' P5  ----------'/'       LIN. MOM. CROSS FLOW'/'    IN
     1 ORDER OF CONSECUTIVE NUMBER OF THE SUBCH. BOUNDARIES' /)
  860 FORMAT('0',' P6  ----------'/'       INV OF MIXING DISTANCE'/'  IN
     1 ORDER OF CONSECUTIVE NUMBER OF THE SUBCH. BOUNDARIES' /)
  870 FORMAT('0','       ***INTERMEDIATE RESULTS *** ')
  880 FORMAT('0',5X,2E15.7,5X,E15.7)
  890 FORMAT('0',5X,I3,3E15.7//)
  950 FORMAT('0',' P7 ----------'/'       WIJ'/)
  960 FORMAT('0',' P8 ----------'/'        BETA'/)
      GO TO 11
      STOP
      END
```

Input Data
Case #4

```
  0    0    1    0
5  7  4  1
1  2  3  7
4  5  6
1  2  3  4
2  3  4  5

 7  7  8
12 12 13
13 12 13
 7  7  7
13 12 13
13 12 13
13 12 13
0.25
0.179          0.230
1.25
0.0            0.02
0.0504         0.0416667      0.0416667      0.0416667      0.0416667
0.0416667      0.0416667
0.005

1.0
73.6           151.           153.           154.
 0.62207470D 00 0.70074208D 00 0.75037571D 00 0.78703504D 00 0.81486774D 00
 0.83473975D 00 0.84626198D 00
 0.60486418D 00 0.68151183D 00 0.72985073D 00 0.76560988D 00 0.79291384D 00
 0.81270035D 00 0.82466675D 00
 0.60099100D 00 0.67680133D 00 0.72453947D 00 0.75999024D 00 0.78745788D 00
 0.80812768D 00 0.82192974D 00 0.82835770D 00
 0.78746871D 00 0.87761388D 00 0.93271047D 00 0.97321539D 00 0.10054220D 01
 0.10320100D 01 0.10542793D 01 0.10728742D 01 0.10880837D 01 0.10999928D 01
 0.11085765D 01 0.11137658D 01
 0.79002269D 00 0.88072400D 00 0.93625480D 00 0.97711108D 00 0.10095778D 01
 0.10363082D 01 0.10585639D 01 0.10769432D 01 0.10916854D 01 0.11028297D 01
 0.11103165D 01 0.11140617D 01
 0.79674968D 00 0.88779273D 00 0.94343112D 00 0.98433181D 00 0.10168542D 01
 0.10437076D 01 0.10662080D 01 0.10850098D 01 0.11004082D 01 0.11124926D 01
 0.11212401D 01 0.11265827D 01 0.11284566D 01
```

| | | | | |
|---|---|---|---|---|
| 0.80388672D 00 | 0.89561734D 00 | 0.95166996D 00 | 0.99287297D 00 | 0.10256366D 01 |
| 0.10526932D 01 | 0.10753714D 01 | 0.10943334D 01 | 0.11098796D 01 | 0.11221031D 01 |
| 0.11309829D 01 | 0.11364517D 01 | 0.11384454D 01 | | |
| 0.80155753D 00 | 0.89339085D 00 | 0.94961014D 00 | 0.99097150D 00 | 0.10238408D 01 |
| 0.10509064D 01 | 0.10734483D 01 | 0.10920748D 01 | 0.11070307D 01 | 0.11183581D 01 |
| 0.11259982D 01 | 0.11298664D 01 | | | |
| 0.80507078D 00 | 0.89692972D 00 | 0.95306427D 00 | 0.99432878D 00 | 0.10271408D 01 |
| 0.10542350D 01 | 0.10769404D 01 | 0.10959182D 01 | 0.11114677D 01 | 0.11236802D 01 |
| 0.11325335D 01 | 0.11379595D 01 | 0.11398940D 01 | | |
| 0.61477291D 00 | 0.69168006D 00 | 0.73964310D 00 | 0.77438204D 00 | 0.79988183D 00 |
| 0.81696060D 00 | 0.82533485D 00 | | | |
| 0.62539813D 00 | 0.70367336D 00 | 0.75250198D 00 | 0.78774343D 00 | 0.81331174D 00 |
| 0.82989551D 00 | 0.83711601D 00 | | | |
| 0.64363938D 00 | 0.72372277D 00 | 0.77367111D 00 | 0.80981139D 00 | 0.83625063D 00 |
| 0.85379719D 00 | 0.86212742D 00 | | | |
| 0.78703945D 00 | 0.87709451D 00 | 0.93212113D 00 | 0.97256917D 00 | 0.10047328D 01 |
| 0.10312953D 01 | 0.10535620D 01 | 0.10721840D 01 | 0.10874575D 01 | 0.10994746D 01 |
| 0.11082158D 01 | 0.11136152D 01 | 0.11156100D 01 | | |
| 0.78982923D 00 | 0.88049447D 00 | 0.93599801D 00 | 0.97683257D 00 | 0.10092834D 01 |
| 0.10360050D 01 | 0.10582614D 01 | 0.10766535D 01 | 0.10914236D 01 | 0.11026133D 01 |
| 0.11101650D 01 | 0.11139951D 01 | | | |
| 0.79670240D 00 | 0.88773726D 00 | 0.94336955D 00 | 0.98426535D 00 | 0.10167840D 01 |
| 0.10436351D 01 | 0.10661350D 01 | 0.10849384D 01 | 0.11003413D 01 | 0.11124334D 01 |
| 0.11211924D 01 | 0.11265504D 01 | 0.11284437D 01 | | |
| 0.80420871D 00 | 0.89600576D 00 | 0.95210981D 00 | 0.99335459D 00 | 0.10261499D 01 |
| 0.10532252D 01 | 0.10759055D 01 | 0.10948480D 01 | 0.11103478D 01 | 0.11224928D 01 |
| 0.11312582D 01 | 0.11365742D 01 | 0.11383769D 01 | | |
| 0.80167405D 00 | 0.89353156D 00 | 0.94976955D 00 | 0.99114592D 00 | 0.10240261D 01 |
| 0.10510975D 01 | 0.10736382D 01 | 0.10922544D 01 | 0.11071890D 01 | 0.11184820D 01 |
| 0.11260731D 01 | 0.11298774D 01 | | | |
| 0.80520651D 00 | 0.89709104D 00 | 0.95324504D 00 | 0.99452524D 00 | 0.10273492D 01 |
| 0.10544507D 01 | 0.10771573D 01 | 0.10961287D 01 | 0.11116622D 01 | 0.11238474D 01 |
| 0.11326607D 01 | 0.11380331D 01 | 0.11399003D 01 | | |
| 0.80613414D 00 | 0.89810435D 00 | 0.95430880D 00 | 0.99562540D 00 | 0.10284786D 01 |
| 0.10556055D 01 | 0.10783358D 01 | 0.10973308D 01 | 0.11128890D 01 | 0.11251009D 01 |
| 0.11339438D 01 | 0.11393488D 01 | 0.11412517D 01 | | |
| 0.80320532D 00 | 0.89520860D 00 | 0.95153389D 00 | 0.99297386D 00 | 0.10259051D 01 |
| 0.10530201D 01 | 0.10756002D 01 | 0.10942536D 01 | 0.11092246D 01 | 0.11205542D 01 |
| 0.11281830D 01 | 0.11320259D 01 | | | |
| 0.80639641D 00 | 0.89839258D 00 | 0.95461289D 00 | 0.99594115D 00 | 0.10288036D 01 |
| 0.10559382D 01 | 0.10786749D 01 | 0.10976752D 01 | 0.11132378D 01 | 0.11254531D 01 |
| 0.11342985D 01 | 0.11397049D 01 | 0.11416084D 01 | | |
| 0.738411D 00 | 0.963854D 00 | 0.105534D 01 | 0.106058D 01 | 0.106166D 01 |